The University of Alberta
Printing Department
Edmonton, Alberta

THE UNIVERSITY OF ALBERTA

INSTABILITY OF THIN SHALLOW CLAMPED ARCHES

by

© ANAND S. AGGARWAL

A THESIS

SUBMITTED TO THE FACULTY OF GRADUATE STUDIES

IN PARTIAL FULFILMENT OF THE REQUIREMENTS FOR THE DEGREE

OF MASTER OF SCIENCE

DEPARTMENT OF MECHANICAL ENGINEERING

EDMONTON, ALBERTA

FALL, 1969

UNIVERSITY OF ALBERTA

FACULTY OF GRADUATE STUDIES

The undersigned certify that they have read, and recommend to the Faculty of Graduate Studies for acceptance, a thesis entitled "INSTABILITY OF THIN SHALLOW CLAMPED ARCHES" submitted by ANAND S. AGGARWAL in partial fulfilment of the requirements for the degree of Master of Science.

ABSTRACT

An experimental and theoretical analysis of a light shallow clamped arch under a central concentrated load is performed. Arches covering a wide range of arch geometry are considered. It is shown theoretically that arch weight has significant effect on large deflections. Results of experiments conducted are in good agreement with theoretical results.

ACKNOWLEDGMENTS

The author wishes to thank

- Dr. J.S. Kennedy for his guidance and supervision of this thesis
- The staff members of the Mechanical Engineering Shop for their help in experimental work
- Mr. J.N. Welling, Drs. J.M. Chudobiak and G. deVries for their suggestions
- Miss H. Wozniuk for her patience in typing
- The National Research Council of Canada (Grant NRC A-4762) and the University of Alberta for financial support.

TABLE OF CONTENTS

LIST OF TABLES

LIST OF FIGURES

NOTATION

E	Young's modulus
F_o	force at the point of loading
$\overline{F}$	$= F_o R_o^2/EI$
H	rise of circular arch
I	moment of inertia
M	bending moment at any point
M_o	bending moment at the point of loading
$\overline{M}$	$= M_o R_o/EI$
N_o	normal force at the point of loading
P	applied concentrated radial load
P_U	upper buckling load
P_L	lower buckling load
$\overline{P}_{UN}$	dimensionless upper buckling load $= P_U R_o^2/EI$
$\overline{P}_{LN}$	dimensionless lower buckling load $= P_L R_o^2/EI$
$\overline{P}_{UC}$	dimensionless upper buckling load considering effects of arch weight
$\overline{P}_{LC}$	dimensionless lower buckling load considering effects of arch weight
Q_o	shearing force at the point of loading
R	radius of curvature in the distorted state
R_o	radius of circular arch

s	length of arch
$\bar{s}$	$= s/R_o$
t	thickness of arch
β	angle between X axis and the line of action of F_o
ϕ	angle between Y axis and the normal at S
ϕ_o	ϕ in the undistorted state
Ω	semi-angle of circular arch
δ	central deflection
$\bar{\delta}$	$= \delta/R_o$
ρ	weight per unit length of the arch
$\bar{\rho}$	$= \rho R_o^3/EI$
ρ_W	$= \bar{\rho}/\bar{P}_{UN}$
ρ_U	$= \bar{P}_{UC}/\bar{P}_{UN}$
ρ_L	$= \bar{P}_{LC}/\bar{P}_{UN}$
λ	$= R_o\Omega^2/t$

Other symbols are defined when used.

CHAPTER I

INTRODUCTION

The shallow arch represents one of the simplest realistic structures from which most of the features of elastic instability theory can be illustrated. The study of this subject gives a better insight to the more complicated problem of buckling of shells which has presented a challenge to engineers for many years.

1.1 Definition of Buckling Load

Instability in the case of shallow arches is caused by the load reaching a maximum as illustrated in Figure 1.1, a typical load-deflection curve for a shallow arch. The load-deflection curve implies that there exist three possible states of equilibrium for each load in the range $P_L < P < P_U$ and only one equilibrium state for each load outside this interval. The points on the branch OA of the curve correspond to unbuckled states, those on the branch BC to buckled states, and those on the segment AB to unstable states. The arch buckles at some load in the interval $P_L \leq P \leq P_U$ and hence P_L and P_U are called the lower and upper buckling loads respectively.

1.2 Review of Related Work

Buckling of shallow arches under concentrated radial load has been investigated by two different non-linear methods.

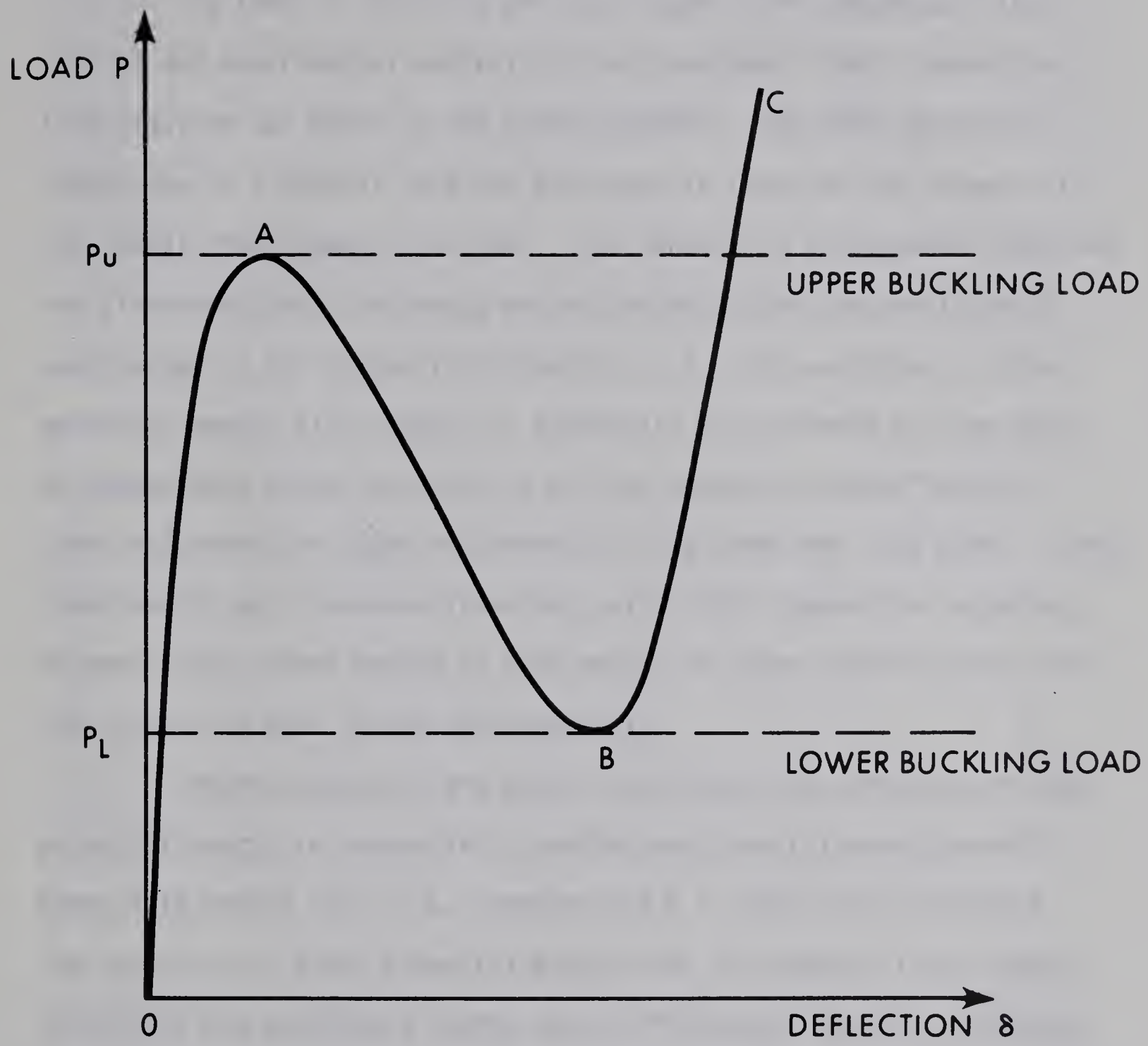

FIGURE 1.1 A TYPICAL LOAD-DEFLECTION CURVE FOR A SHALLOW ARCH

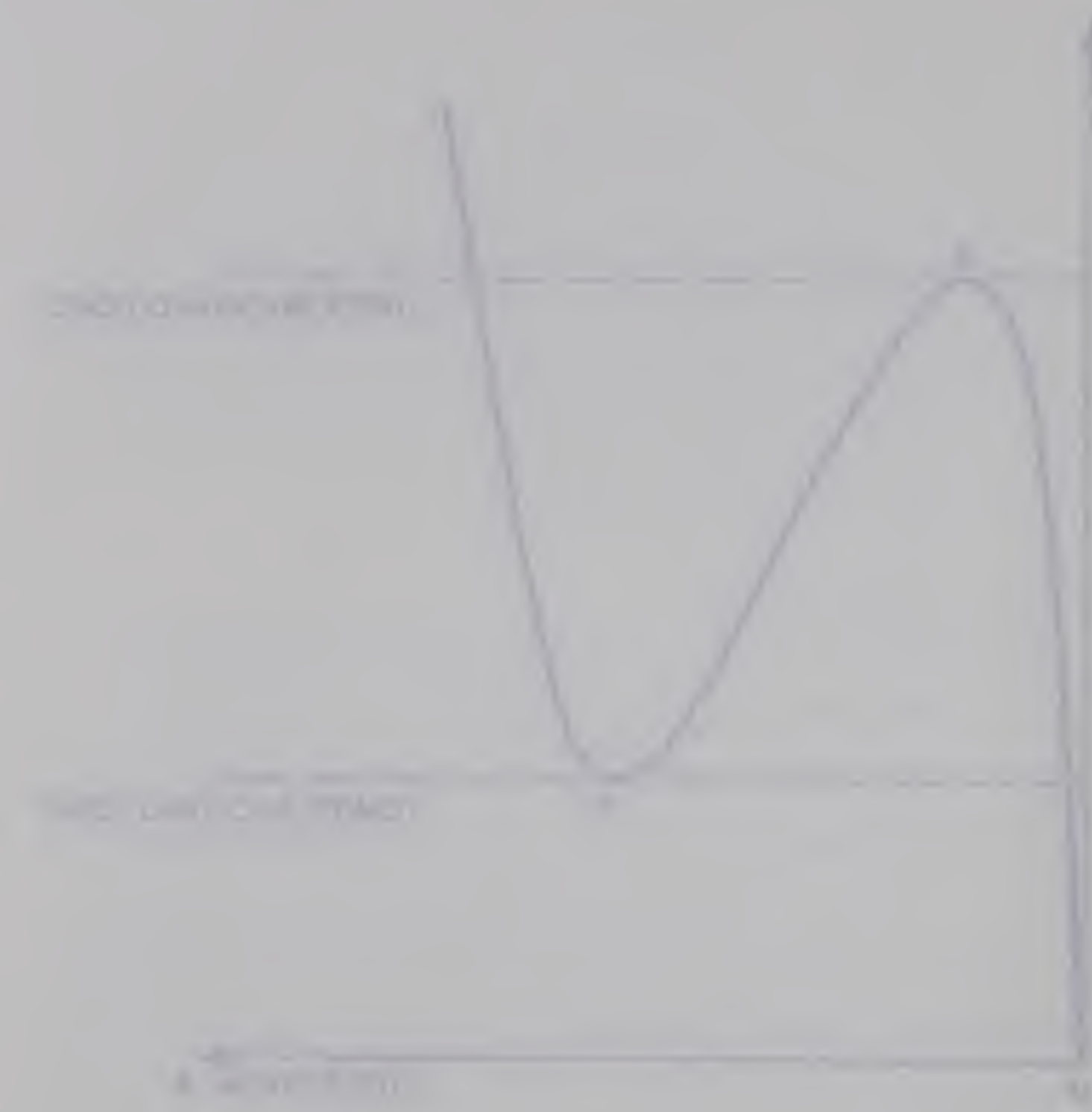

1.2.1 Energy Criterion

In 1962, A. Gjelsvik and S.R. Bodner (4)* presented a theoretical and experimental analysis of this problem. Their theoretical investigation was based on the energy methods. The total potential energy due to a central load was expressed in terms of the tangential and radial displacement functions. The tangential displacement function was eliminated from the energy expression employing the condition of equilibrium in the tangential direction, i.e., the variation of total potential energy with respect to tangential displacement must be zero. An approximate series solution to get the complete load-deflection curve and hence the upper and lower buckling loads was also given. Their experimental work compared favourably with their theoretical solution. However, only arches having an arch weight to upper buckling load ratio less than 0.05 were tested experimentally.

Whereas Gjelsvik and Bodner considered the variation of total potential energy in tangential direction and then followed the well known Ritz Method (10), H.L. Schreyer and E.F. Masur (9) considered the variation of total potential energy both in tangential and radial directions and obtained a fourth order differential equation relating load and deflection. An exact solution to this equation was also given. They considered both symmetrical and antisymmetrical modes of deformation and found that under concentrated load at the center, the arch remains symmetrical until after upper buckling load P_U and though un-

---

*Numbers in parentheses refer to references in Bibliography.

symmetrical in the unstable region, returns to a symmetrical configuration when stability is again attained, as illustrated in Figures 1.2 - 1.4. Hence for this problem the symmetrical buckling criterion governs regardless of arch geometry.

1.2.2 Elastica Approach

J.S. Kennedy (6) derived a non-linear differential equation to satisfy the geometrical conditions and the equilibrium state of the arch using the general theory of the elastica (7). This was subsequently solved for symmetrical deformations by algebraic transformations and the introduction of elliptic integrals. Kennedy also conducted a series of experiments with light, thin, circular arches which were induced to buckle symmetrically by clamping the centre of the arch. The arch centre, therefore, was allowed to move only in the vertical direction and a horizontal tangent at that point was maintained. For a given subtended angle of the arch the application of Kennedy's theory resulted in only one load-deflection curve for non-dimensional plotting whereas he obtained several different, although similar, curves experimentally by employing various arch geometries. Poor arch clamping was suggested as the reason of this discrepancy.

Later in 1963, D.A. Burns (2) undertook an experimental investigation of shallow arches under a concentrated load. He tested a number of light clamped arches and found that in some cases there was as much as 35% deviation from the theoretical curves obtained by the application of Kennedy's or Bodner's theory. The arch specimens tested by

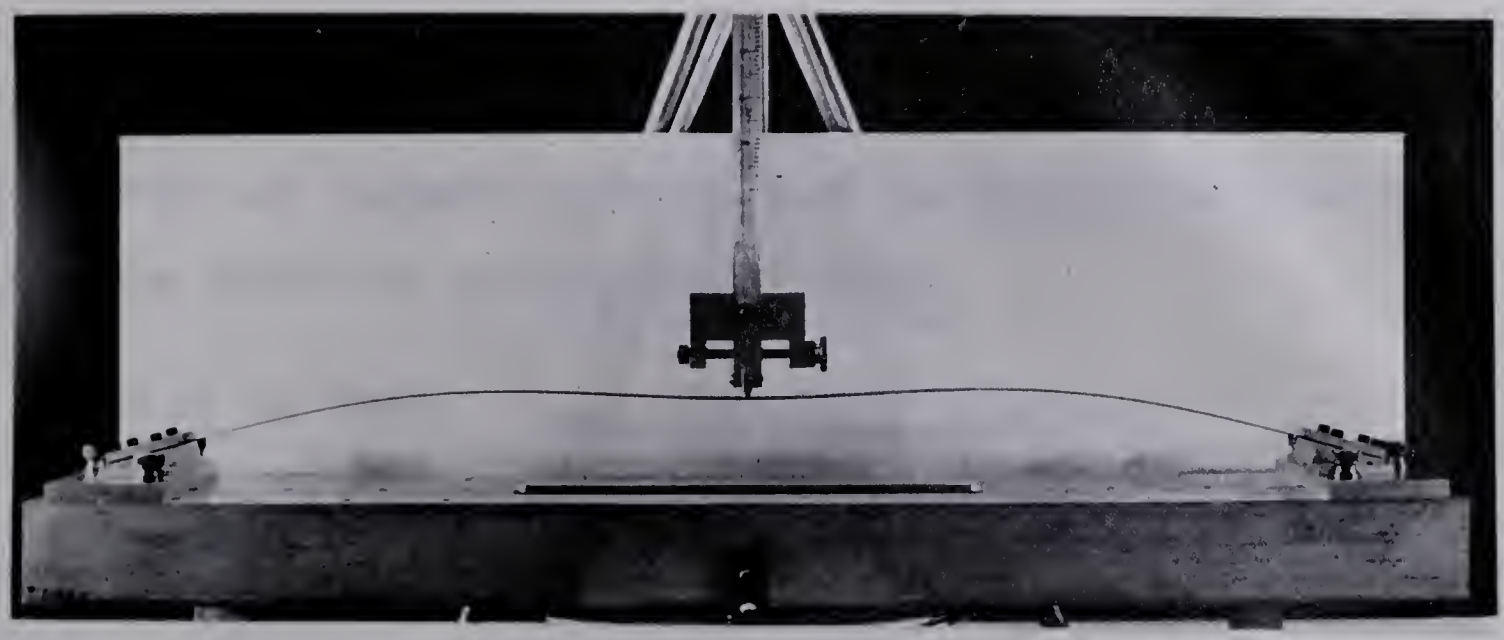

FIGURE 1.2 ARCH IN UNBUCKLED STATE, RETAINING SYMMETRY.

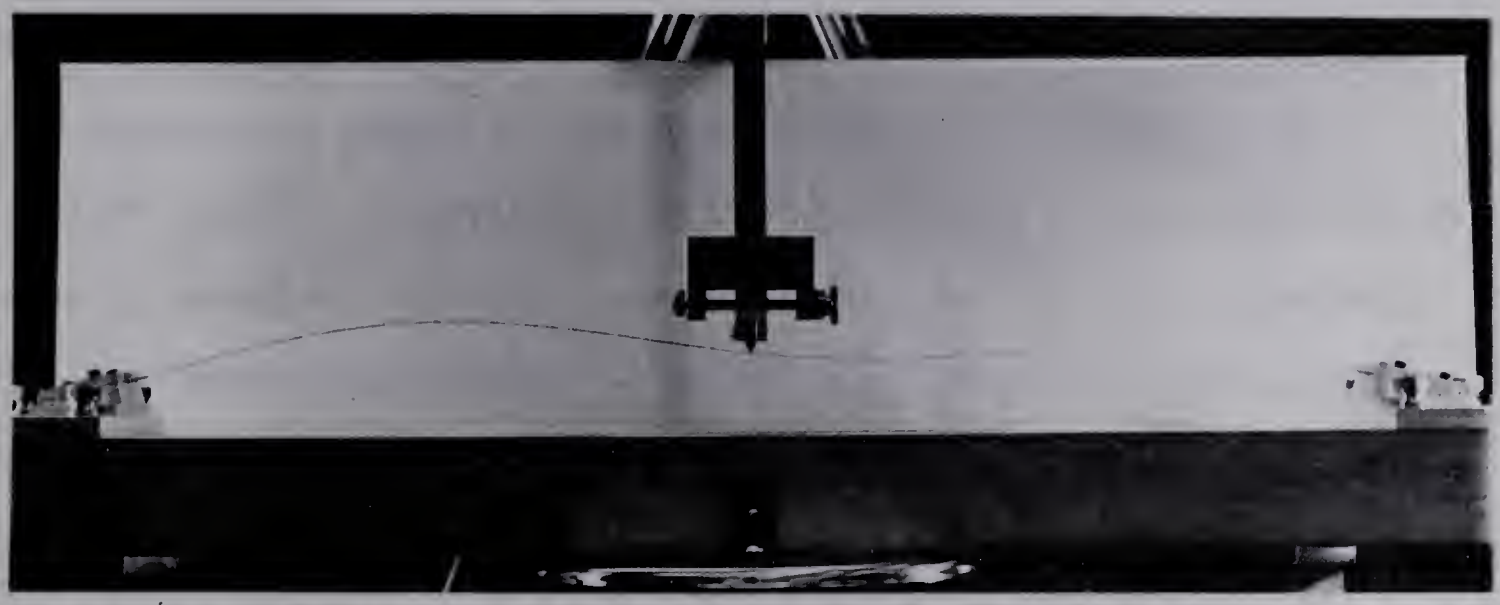

FIGURE 1.3 ARCH IN UNSTABLE STATE, SHOWING PRONOUNCED ASYMMETRY.

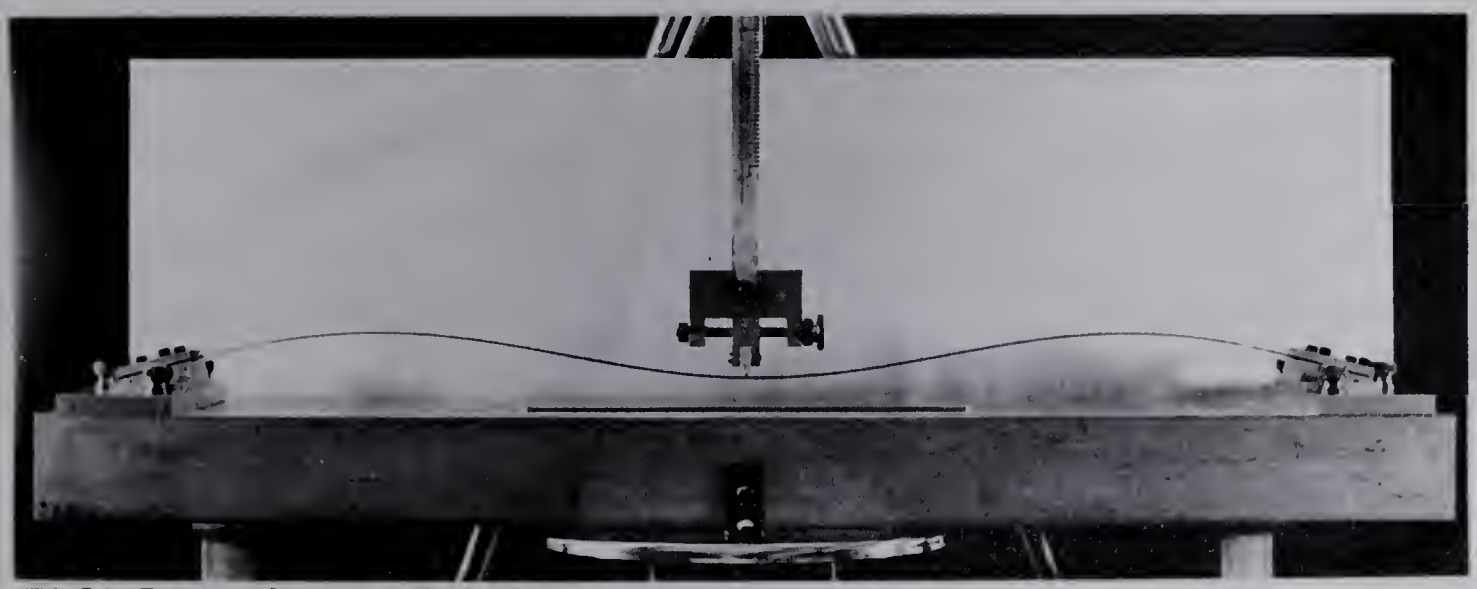

FIGURE 1.4 ARCH IN BUCKLED STATE, SHOWING RETURN TO SYMMETRY

Burns had weight to upper buckling load ratios from 0.06 to 0.48. Arch weight was suggested as the cause of the large discrepancies between the theoretical and experimental curves.

1.3 Aim of the Thesis

In the present work, Burn's line of thought, i.e., weight of the arch does have an effect on the buckling load, has been investigated further. A non-linear differential equation using the elastica approach (7) and taking the arch weight into consideration has been derived. The equation developed has been solved to obtain complete load-deformation curves by numerical techniques described in Appendices A and B. Experiments on arches covering a wide range of arch geometry have been conducted and the results are in close agreement with the theoretical curves. A linear correlation has been observed between the arch weight to upper buckling load ratio and non-dimensionlised upper and lower buckling loads.

CHAPTER II

THEORETICAL ANALYSIS

The elastica approach employed to study the large deflections of flexible bars is well known (7). This method is used here to analyse the symmetrical mode of deformation of a ring segment of radius R_o, having built in ends which subtend an angle 2Ω, loaded by a radial load P directed along the line of symmetry as shown in Figure 2.1. The plane of loading, i.e., the plane defined by the applied load and the reactive forces, contains one principal axis of inertia of each section, so that the bending of the arch is confined to that plane only.

2.1 Derivation of Governing Equation

Because of the symmetry, only one half of the arch need be considered in the development of the governing differential equation for the problem. As shown in Figure 2.2, at the mid point S_o, the load will consist of a couple M_o, a horizontal compressive force N_o and a vertical shearing force Q_o, and at some other point S of such a couple and a force as to provide equilibrium. A coordinate system X,Y with its origin at the load point S_o, the X axis coinciding with the tangent at S_o and the Y axis coinciding with the normal at S_o and lying along the radius of curvature will be employed. The forces N_o and Q_o acting at the point S_o can be replaced by a single force F_o acting along a

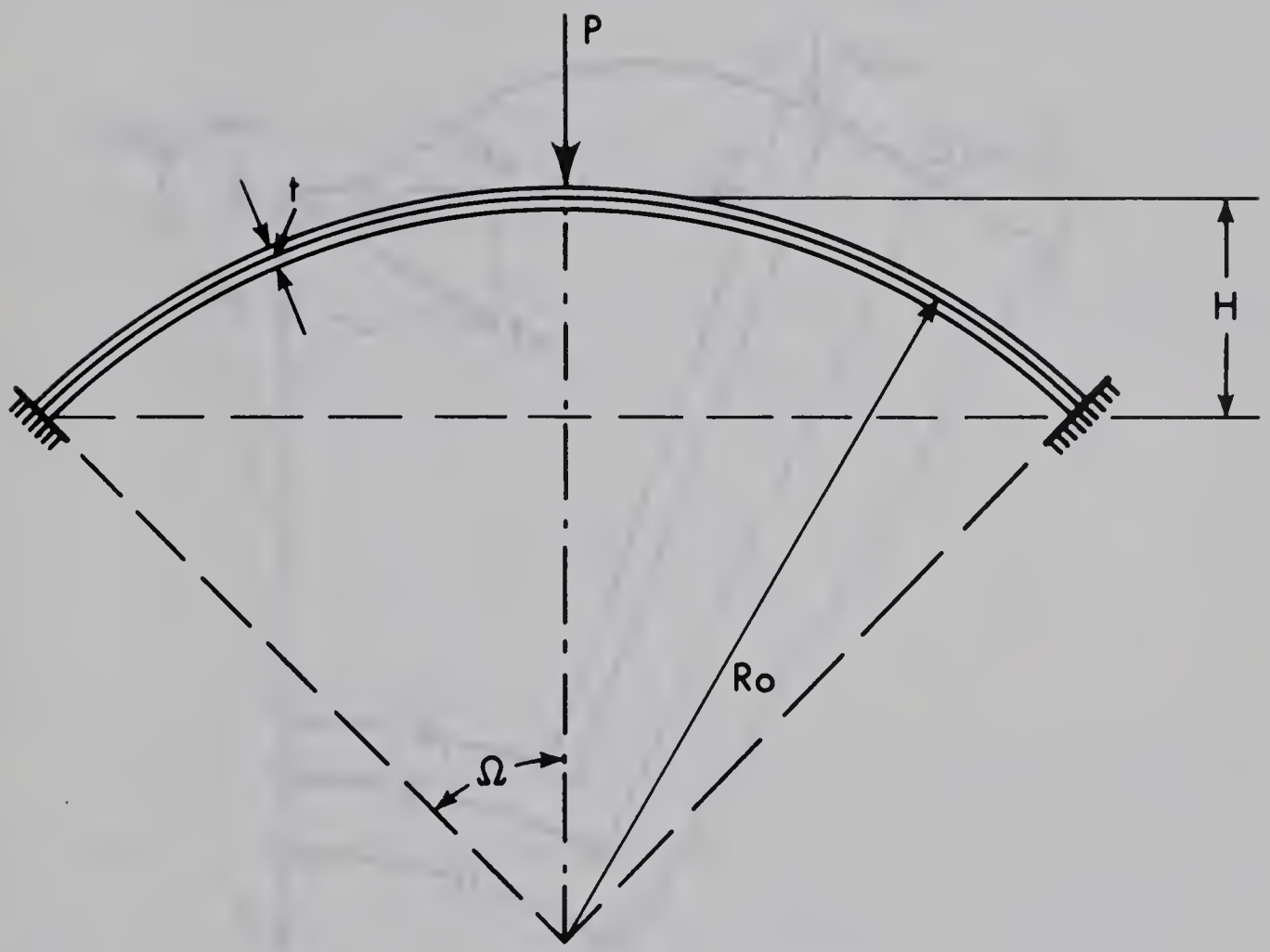

FIGURE 2.1 CLAMPED CIRCULAR ARCH UNDER CONCENTRATED LOAD

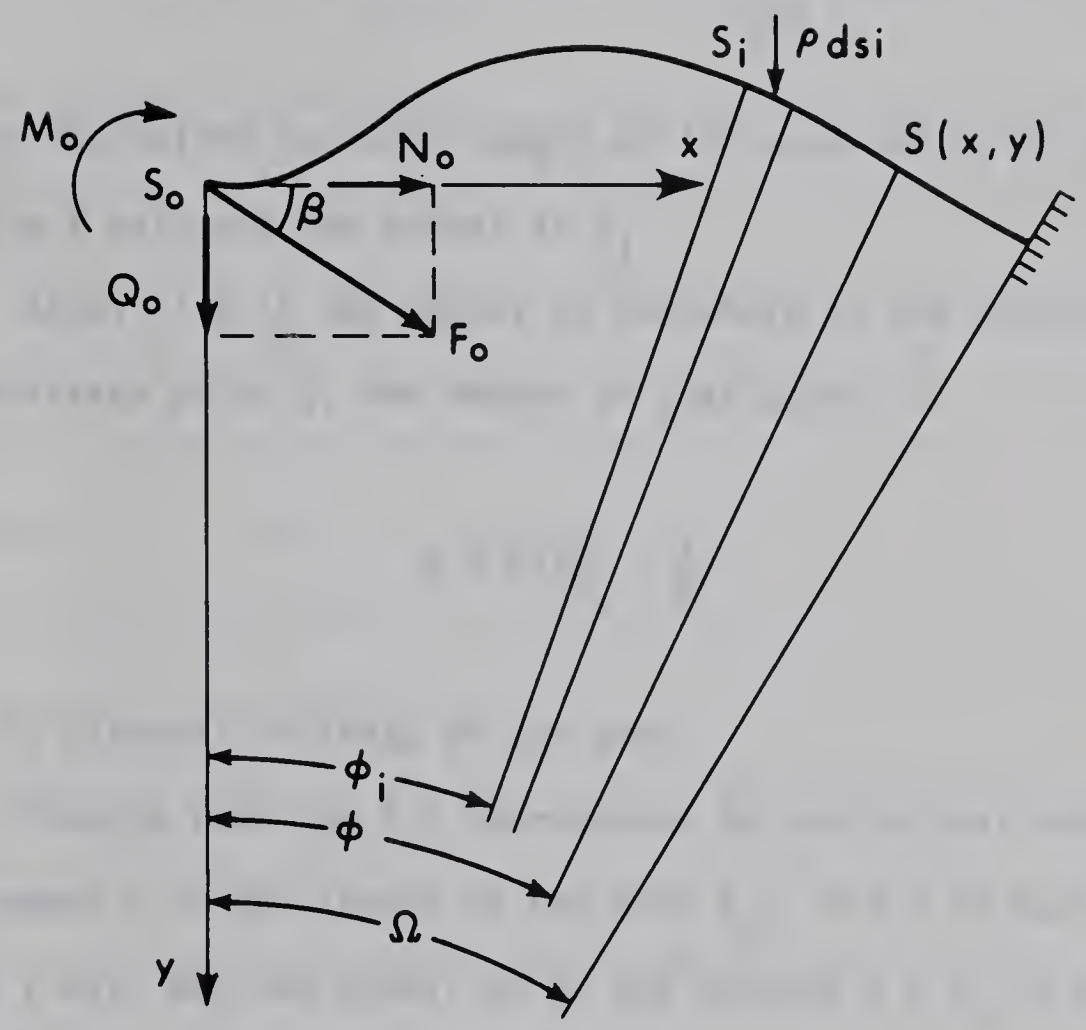

FIGURE 2.2 SEMI-ARCH AFTER DEFORMATION

line which makes an angle β with the X axis.

The bending moment at an arbitrary point is defined as positive if it tends to decrease the curvature. From equilibrium the moment M, at any point S, on the curve is given by

$$M = M_o - F_o(x\sin\beta - y\cos\beta) - \int_{x_i=0}^{x_i=x} \frac{\rho(x-x_i)}{\cos\phi_i}\, dx_i \qquad 2.1$$

where ρ is the weight per unit length of the arch and ϕ_i is the angle between the Y axis and the normal at S_i .

Also, if R is the radius of curvature in the distorted state at the arbitrary point S, the moment at that point is

$$M = EI\left(\frac{1}{R_o} - \frac{1}{R}\right) \qquad 2.2$$

where EI is flexural rigidity of the arch.

Passing from the X,Y coordinates to the natural coordinates s and ϕ, where s is the length of the arch S_oS, and ϕ is the angle between the Y axis and the normal at S, and letting $\phi = \phi_o$ in the undistorted state, there exist the relations

$$\frac{1}{R} = \frac{d\phi}{ds} \qquad \frac{1}{R_o} = \frac{d\phi_o}{ds}$$

$$\frac{dx}{ds} = \cos\phi \qquad \frac{dy}{ds} = \sin\phi \qquad 2.3$$

Employing Equations 2.2 and 2.3; Equation 2.1 becomes

$$EI\left(\frac{d\phi_o}{ds} - \frac{d\phi}{ds}\right) = M_o - F_o(x\sin\beta - y\cos\beta) - \int_{x_i=0}^{x_i=x} \frac{\rho(x-x_i)}{\cos\phi_i}\, dx_i \qquad 2.4$$

The slope of the tangent ϕ_i, is a complicated function of the loading. Therefore, the last term in Equation 2.4 which accounts for the direct contribution of the arch weight to the bending moment becomes difficult if not impossible to evaluate. To simplify the situation, let us restrict our attention to shallow arches, i.e., arches in which the ratio of height H, to radius of curvature R_o, is less than 0.1. For such cases, in evaluating the last term of Equation 2.4, it is reasonable to employ the approximation that each point on the arch moves vertically. This means that the value of the last term of Equation 2.4 at a section will always be the same regardless of the arch deformation. Consequently, the bending moment due to the arch weight can be evaluated with respect to the undistorted state.

Let $\tilde{X}$, $\tilde{Y}$ be the coordinate axes fixed to the undistorted shape of the arch and ϕ_o be the angle between the $\tilde{Y}$ axis and the normal to S, as shown in Figure 2.3. Then the last term in the Equation 2.4 can be written as

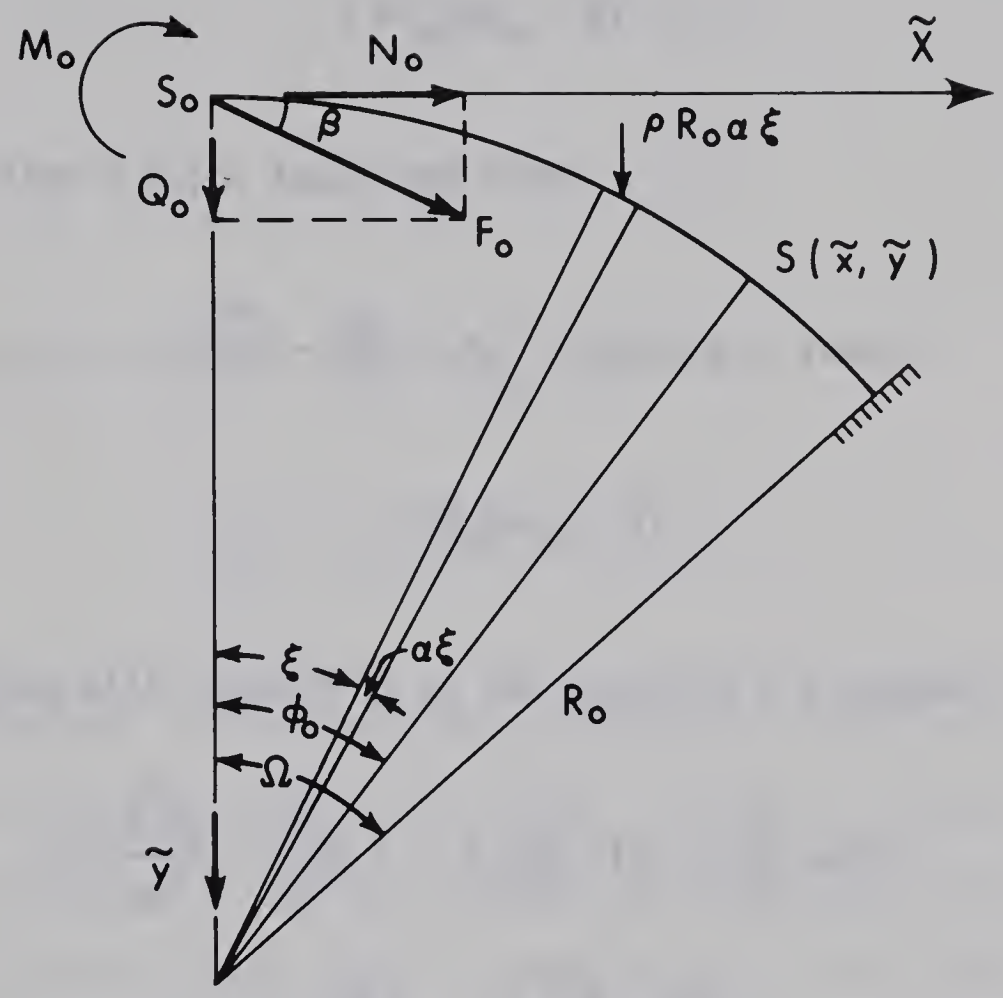

FIGURE 2.3 SEMI-ARCH BEFORE DEFORMATION

$$\int_{\xi=0}^{\xi=\phi_o} \rho R_o(\tilde{x} - R_o \sin\xi)\, d\xi$$

$$= [\rho R_o(\tilde{x}\xi + R_o \cos\xi)]_{\xi=0}^{\xi=\phi_o}$$

$$= \rho R_o(\tilde{x}\phi_o - \tilde{y})$$

and the Equation 2.4 now takes the form

$$EI\left(\frac{d\phi_o}{ds} - \frac{d\phi}{ds}\right) = M_o - F_o(x\sin\beta - y\cos\beta)$$

$$- \rho R_o(\tilde{x}\phi_o - \tilde{y}) \qquad 2.5$$

Differentiating with respect to s, the Equation 2.5 becomes

$$EI\left(\frac{d^2\phi_o}{ds^2} - \frac{d^2\phi}{ds^2}\right) = - F_o\left(\frac{dx}{ds}\sin\beta - \frac{dy}{ds}\cos\beta\right)$$

$$- \rho R_o\left(\frac{d\tilde{x}}{ds}\phi_o + \tilde{x}\frac{d\phi_o}{ds} - \frac{d\tilde{y}}{ds}\right)$$

Employing the relations 2.3 and noting that the curvature of ring segment is uniform in the unloaded state, i.e., $d\phi_o/ds = 1/R_o$, Equation 2.6 simplifies to

$$- EI\,\frac{d^2\phi}{ds^2} = F_o \sin(\phi-\beta) - \rho R_o \phi_o \cos\phi_o \qquad 2.7$$

Adopting R_o and EI as standards of length and stiffness and defining the dimensionless quantities,

$$\bar{s} = \frac{s}{R_o} \qquad \bar{x} = \frac{x}{R_o}$$

$$\bar{y} = \frac{y}{R_o} \qquad \bar{F} = \frac{F_o R_o^2}{EI}$$

$$\bar{M} = \frac{M_o R_o}{EI} \qquad \bar{\rho} = \frac{\rho R_o^3}{EI}$$

Equation 2.7 can be written in the form

$$\frac{d^2\phi}{d\bar{s}^2} + \bar{F}\sin(\phi-\beta) = \bar{\rho}\,\bar{s}\cos\bar{s} \qquad 2.8$$

Equation 2.8 is the differental equation describing load-deformation characteristics of the system. It may be remarked here that this equation is of the same form as developed by Kennedy (6) but in addition it has an extra term on the right hand side which accounts for the effects of arch weight.

2.2 Boundary Conditions

Since we are analysing the symmetrical mode of deformation of the arch, the tangent at the center must remain horizontal, i.e.,

$$\phi = 0 \quad \text{at} \quad \bar{s} = 0 \qquad 2.9$$

Secondly, because of the fixed ends

$$\phi = \Omega \quad \text{at} \quad \bar{s} = \Omega \tag{2.10}$$

In addition to the above two boundary conditions, the horizontal projection must remain constant and equal to sin Ω, i.e.,

$$\int_0^{\Omega} \frac{d\bar{x}}{d\bar{s}}\, d\bar{s} = \sin \Omega$$

Since

$$\frac{d\bar{x}}{d\bar{s}} = \cos \phi \ ,$$

then

$$\int_0^{\Omega} \cos\phi \, d\bar{s} = \sin \Omega \tag{2.11}$$

A solution to the governing differential equation 2.8 subject to the boundary conditions 2.9 - 2.11 is desired. Once a solution has been obtained, the non-dimensional central deflection δ, at the point of loading is given by

$$\bar{\delta} = \frac{\tilde{y}}{R_o} - \int_0^{\Omega} \frac{d\bar{y}}{d\bar{s}}\, d\bar{s}$$

Since

$$\frac{d\bar{y}}{d\bar{s}} = \sin \phi \ ,$$

then

$$\bar{\delta} = (1 - \cos \Omega) - \int_0^{\Omega} \sin\phi \, d\bar{s}$$

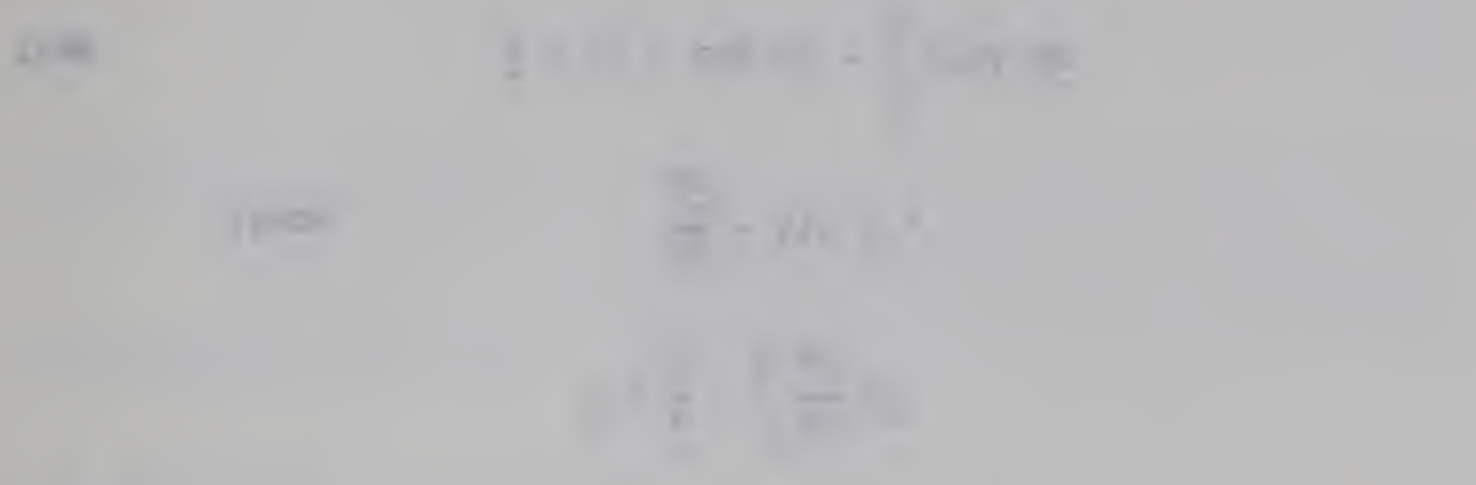

The non-dimensional concentrated load parameter is given by

$$\overline{P} = 2\overline{F} \sin \beta \qquad 2.13$$

2.3 Deflection Under Dead Weight

The central deflection because of the arch dead weight was found by application of the linear theory in form of Castigliano's Theorem.

Considering one half of the arch, Figure 2.3, the moment at any point S, is given by

$$M = M_o + N_o R_o(1-\cos\phi_o) - Q_o R_o \sin \phi_o - \int_{\xi=0}^{\xi=\phi_o} \rho R_o^{\,2}(\sin\phi_o - \sin\xi)\, d\xi \qquad 2.14$$

which on simplification gives

$$M = M_o + N_o R_o(1-\cos\phi_o) - Q_o R_o \sin\phi_o - \rho R_o^{\,2}(\phi_o \sin\phi_o - 1+\cos\phi_o) \qquad 2.15$$

By Castigliano's Theorem

$$\delta M_o = \frac{R_o}{EI} \int_0^{\Omega} M \frac{\partial M}{\partial M_o}\, d\phi_o$$

$$\delta N_o = \frac{R_o}{EI} \int_0^{\Omega} M \frac{\partial M}{\partial N_o}\, d\phi_o \qquad 2.16$$

$$\delta Q_o = \frac{R_o}{EI} \int_0^{\Omega} M \frac{\partial M}{\partial Q_o} d\phi_o$$

are respectively the rotation, the horizontal deflection and the vertical deflection of the center point.

Substituting Equation 2.15 into the Equations 2.16, carrying out the required integration and taking the limit of the resulting expressions as Q_o approaches zero yields,

$$\delta M_o = \frac{R_o}{EI} [M_o\Omega + N_o R_o(\Omega - \sin\Omega)$$

$$- \rho R_o^2(2\sin\Omega - \Omega\cos\Omega - \Omega)] \qquad 2.17$$

$$\delta N_o = \frac{R_o^2}{EI} [M_o(\Omega-\sin\Omega) + N_o R_o(\frac{3\Omega}{2} + \frac{\sin 2\Omega}{4} - 2\sin\Omega)$$

$$- \rho R_o^2(3\sin\Omega - \Omega\cos\Omega - \frac{3}{2}\Omega - \frac{3}{8}\sin 2\Omega + \frac{1}{4}\Omega\cos 2\Omega)] \qquad 2.18$$

$$\delta Q_o = \frac{R_o^2}{EI} [M_o(\cos\Omega-1) + N_o R_o(\cos\Omega - \frac{3}{4} - \frac{\cos 2\Omega}{4})$$

$$+ \rho R_o^2(\frac{\Omega^2}{4} - \frac{1}{4}\Omega\sin 2\Omega - \frac{3}{8}\cos 2\Omega + \cos\Omega - \frac{5}{8})] \qquad 2.19$$

The symmetry of the problem requires that

$$\delta M_o = \delta N_o = 0 \qquad 2.20$$

Therefore from Equations 2.17 and 2.18, M_o and N_o can be found in terms of ρ, Ω, R_o and EI. Knowing the values of M_o and N_o, δQ_o, the central deflection under dead weight, can be calculated. For the arches considered in this thesis, this deflection was found to be negligible, i.e., less than one thousandth of an inch.

CHAPTER III

METHOD OF SOLUTION

3.1 Integration Procedure

The governing differential equation, 2.8, can be written as a system of two simultaneous, first-order differential equations

$$\frac{d\phi}{d\bar{s}} = \alpha$$

$$\frac{d\alpha}{d\bar{s}} = \overline{\rho s} \cos \bar{s} - \bar{F} \sin(\phi-\beta) \qquad 3.1$$

Such systems can usually be solved numerically without difficulty, inspite of non-linear terms, provided that the problem is of the "initial-value type", with ϕ and α known at some "initial" value of $\bar{s}$. In the present case, at the initial point $\bar{s} = 0$, ϕ is zero but α and the angle β, which is dependent on the loading are unknown. To overcome this problem, the author has used a "Shooting Method". The slope α and the angle β are assumed at the initial point, Equations 3.1 are integrated numerically using Gill's modification of the Runge-Kutta fourth order method (Appendix A) and the terminal conditions 2.10 and 2.11 computed. The assumed initial values of α and β are then adjusted iteratively until the boundary conditions are satisfied.

3.2 Block Diagram

The computation procedure is illustrated in the block diagram, Figure 3.1. For convenience, the following notation will be employed.

$$\phi = \phi_o \quad \text{at} \quad \bar{s} = 0$$

$$\phi = \phi_\Omega \quad \text{at} \quad \bar{s} = \Omega$$

$$\alpha = \alpha_o \quad \text{at} \quad \bar{s} = 0 \qquad 3.2$$

The computation scheme incorporates two iterative loops because of the two unknown quantities β and α_o. Corresponding to an assumed value of angle β, let α_1, α_2 be two guesses of the initial α_o, and let $\phi_\Omega(\alpha_1)$, $\phi_\Omega(\alpha_2)$ be two values of ϕ at $\bar{s} = \Omega$ obtained from integrating the differential equations 3.1. Graphically the situation may be presented as in Figures 3.2 and 3.3. In Figure 3.2, the solutions of the initial-value problem are drawn, while in Figure 3.3, $\phi_\Omega(\alpha_o)$ is plotted as a function of α_o. Normally a better approximation to α_o can now be obtained by linear interpolation. The intersection of the line joining P_1 and P_2 with a horizontal line from $\phi_\Omega(\alpha_o) = \Omega$, the required value at $\bar{s} = \Omega$, has as its α_o coordinate

$$\alpha_3 = \alpha_1 + (\alpha_2 - \alpha_1) \frac{\Omega - \phi_\Omega(\alpha_1)}{\phi_\Omega(\alpha_2) - \phi_\Omega(\alpha_1)} \qquad 3.3$$

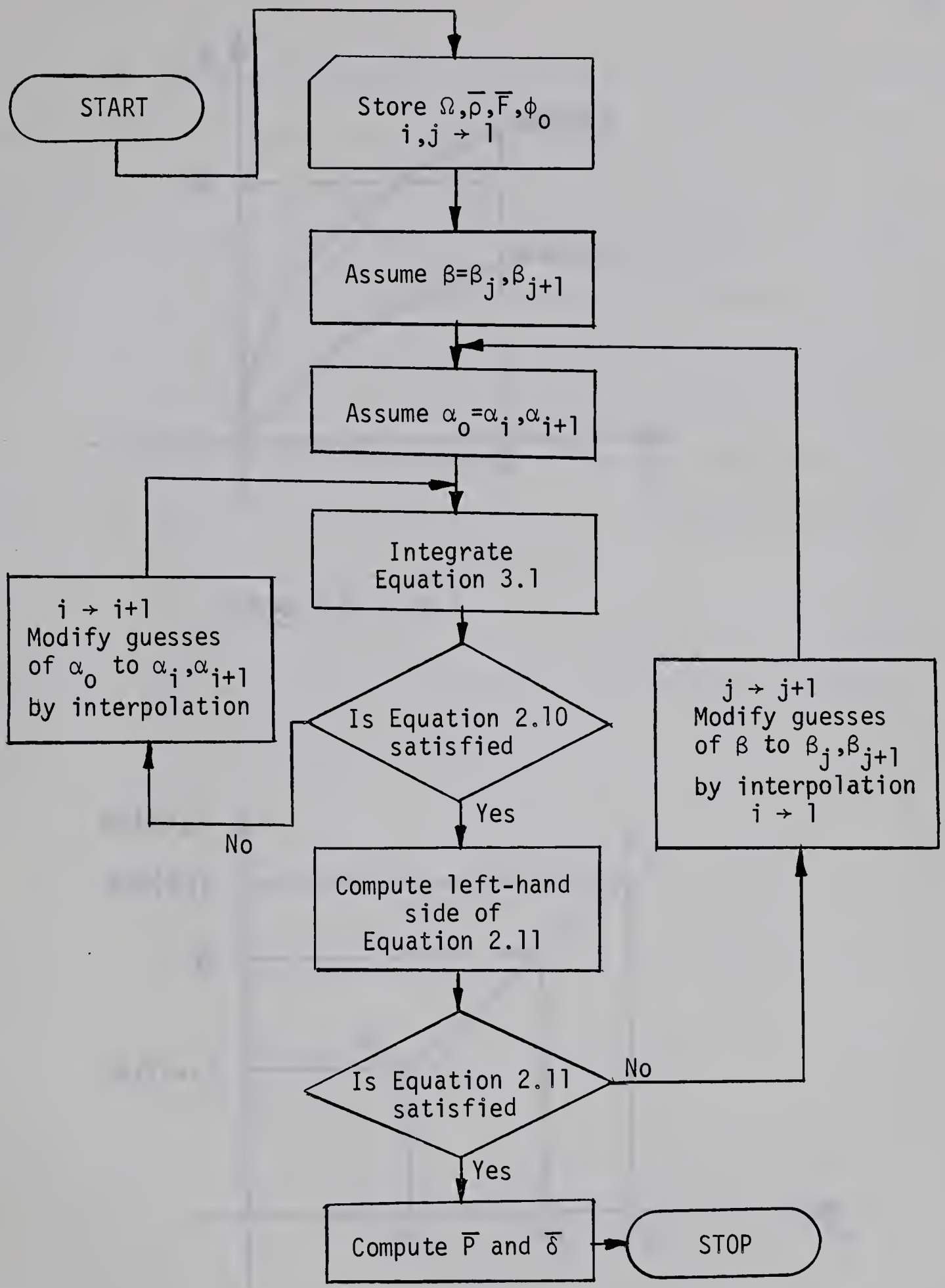

FIGURE 3.1 BLOCK DIAGRAM

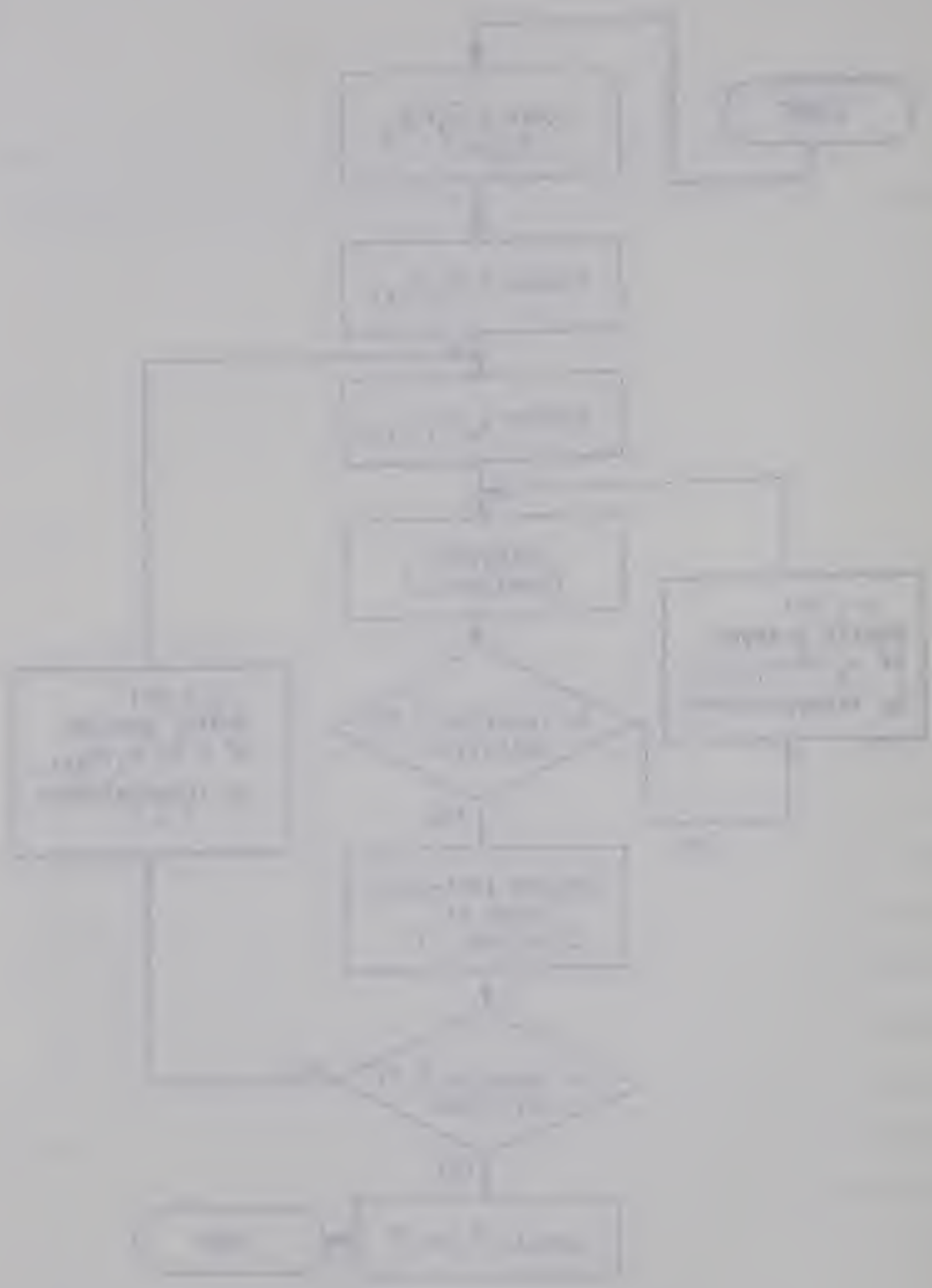

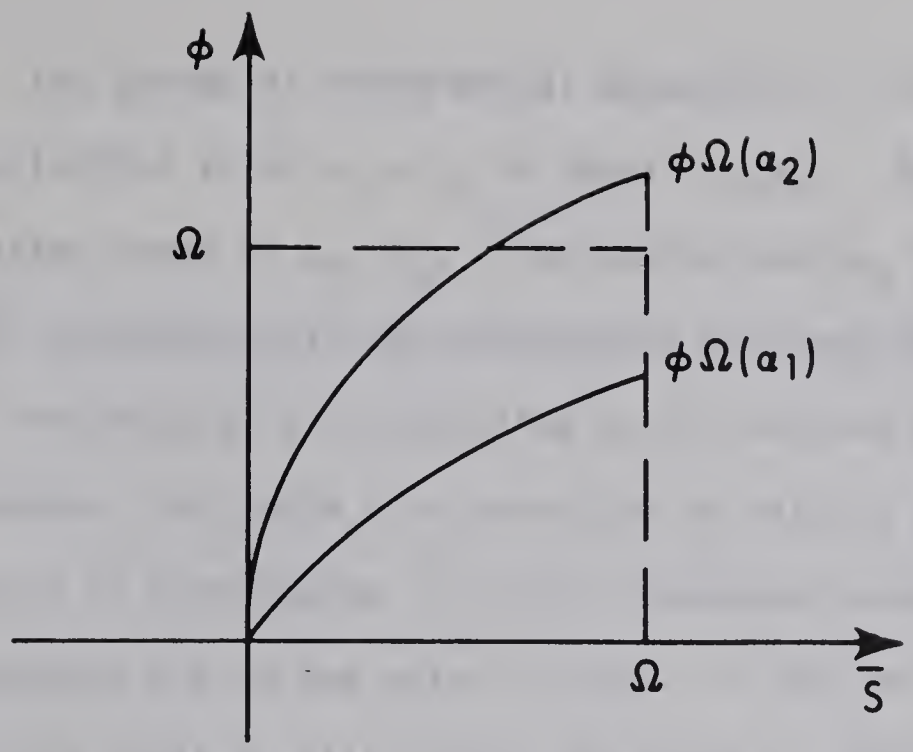

FIGURE 3.2 ϕ vs $\bar{s}$

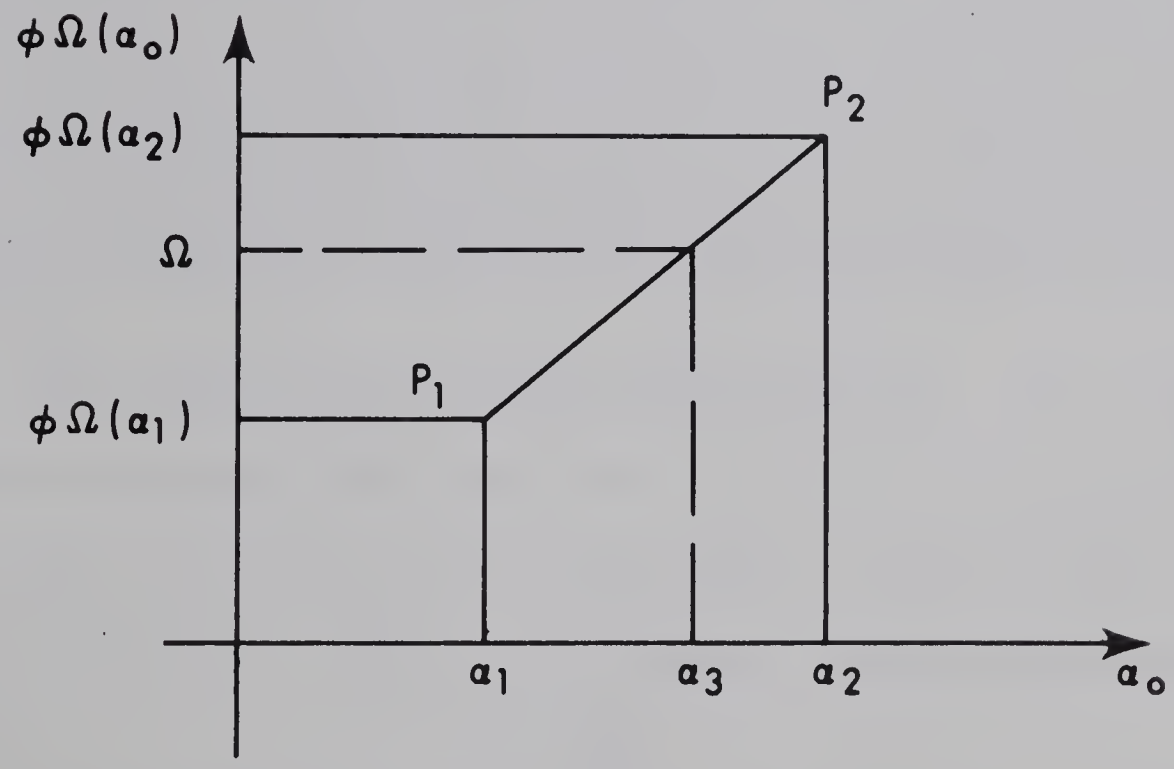

FIGURE 3.3 $\phi_{\Omega}(\alpha_o)$ vs α_o

The system of differential equations 3.1 is now again integrated using the initial value $\alpha_o = \alpha_3$ to obtain $\phi_\Omega(\alpha_3)$. Again using linear interpolation based on α_2, α_3, a new approximate α_4 is obtained. The process is repeated until the convergence has been obtained i.e. the boundary condition 2.10 is satisfied to the desired accuracy. In a similar manner, the angle β is corrected to satisfy the condition 2.11. The rapidity of convergence is clearly dependent upon how close the initial guesses are to the actual values. It may be noted here that any change in the angle β, will change the slope α_o, therefore the inner iterative loop will have to be satisfied again.

The central deflection $\overline{\delta}$, given by the equation 2.12 is then computed by stepwise integration employing a combination of Simpson's and Newton's Three-Eighth Rule (Appendix B).

CHAPTER IV

EXPERIMENTAL PROCEDURE AND APPARATUS

4.1 Apparatus

The experimental apparatus is shown in Figure 4.1.

The arch bed was machined from a length of 65S-T6 6" x 2-3/4" aluminum channel. The top face and the tips of channel flanges were milled in the Department Workshop to ensure that these surfaces would be smooth and parallel to each other. A centre slot was machined out of the top face of the bed as shown in Figure 4.2 to permit large deformations of the arch should this prove necessary during a test. The parallel rows of holes were drilled so that the arch support blocks would be positioned via guide pegs, and would thus be aligned correctly with no further effort. The holes tapped at regular intervals along the channel centerline were placed to mate with the fixing bolt of each support block.

Three sets of support blocks were fabricated. These blocks were milled so that when the clamps were set in position on the arch bed, the slope of the built-in end of the arch would be 10°, 15° and 20° to the horizontal. Details of the support block are depicted in Figure 4.3.

The arch bed was fixed to the scale pan of an Ohaus Triple Beam Balance. The balance had been securely located on a firm wooden bench

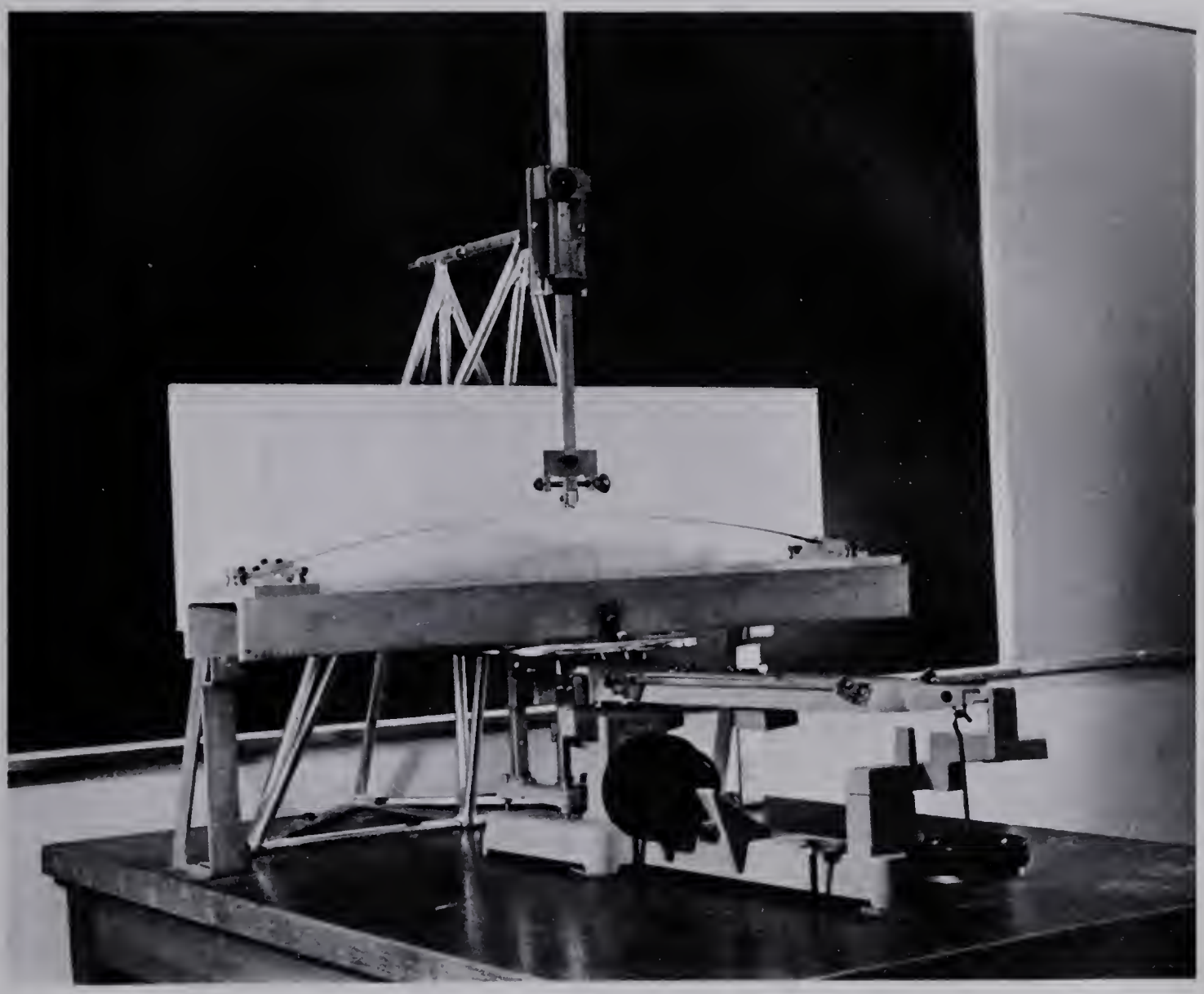

FIGURE 4.1 GENERAL VIEW OF APPARATUS.

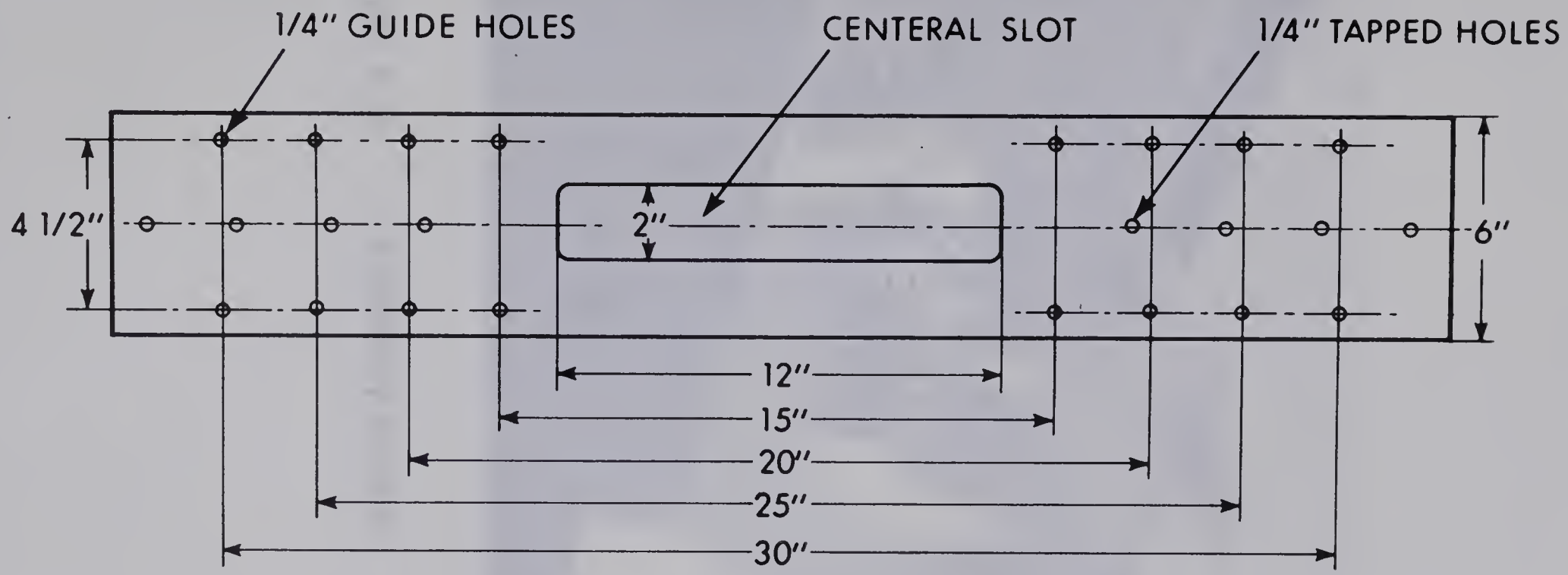

FIGURE 4.2 PLAN VIEW OF ARCH BED

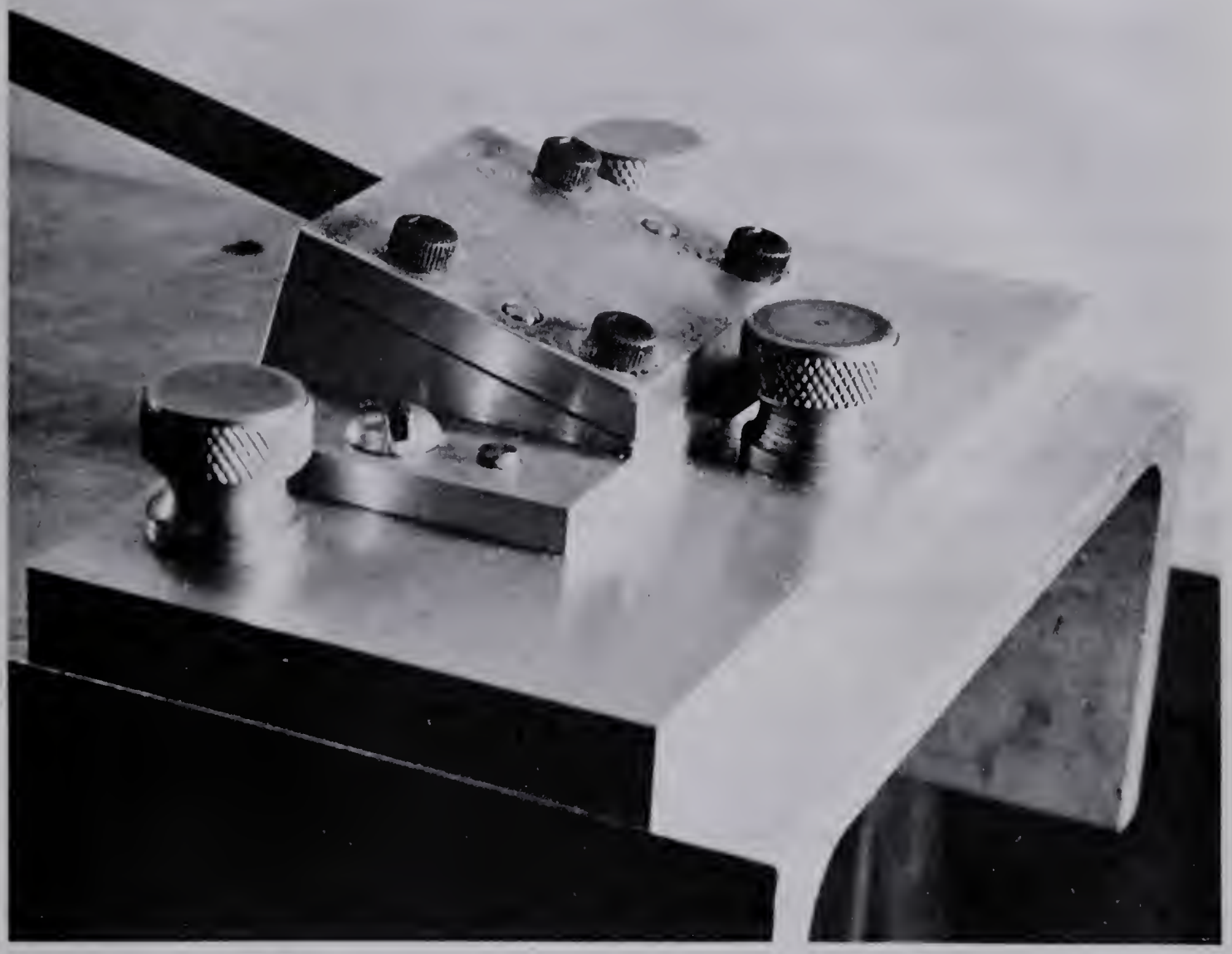

FIGURE 4.3 SUPPORT BLOCK

and shimmed until level. The bed scale system was adjusted carefully and it was checked with a sensitive spirit level to ensure that the upper surface of the arch bed lay in the horizontal plane.

Arch deflections were applied by a loading bar fashioned from a hook gauge, which was supported by a tubular steel frame. A Vernier, with least count 0.012 inch was used with the loading bar. The central point of the arch was allowed to move only in the vertical direction and the tangent at the midpoint was maintained horizontal by the arrangement shown in Figures 4.4 and 4.5.

Prior to its installation, the Ohaus Triple Beam Balance was calibrated, using weights supplied with an analytical balance, accurate to a milligram. It was found to be within the specified tolerance of one gram.

4.2 Test Specimens

The arch test-pieces were cut from banding steel 0.015 or 0.026 inch thick and 0.75 inch wide. The required length was calculated from the specified angle and radius of curvature of the arch. Centre-lines were scribed on each piece to correspond to similar marks on the supporting blocks thereby assisting in the alignment. The black finish of the banding steel lent itself readily to this process. Each length was carefully inspected for imperfections and kinks prior to testing. The circularity of the arch was further insured by measuring the rise of the arch by a Vernier Height Gauge accurate to one thousandth of an inch.

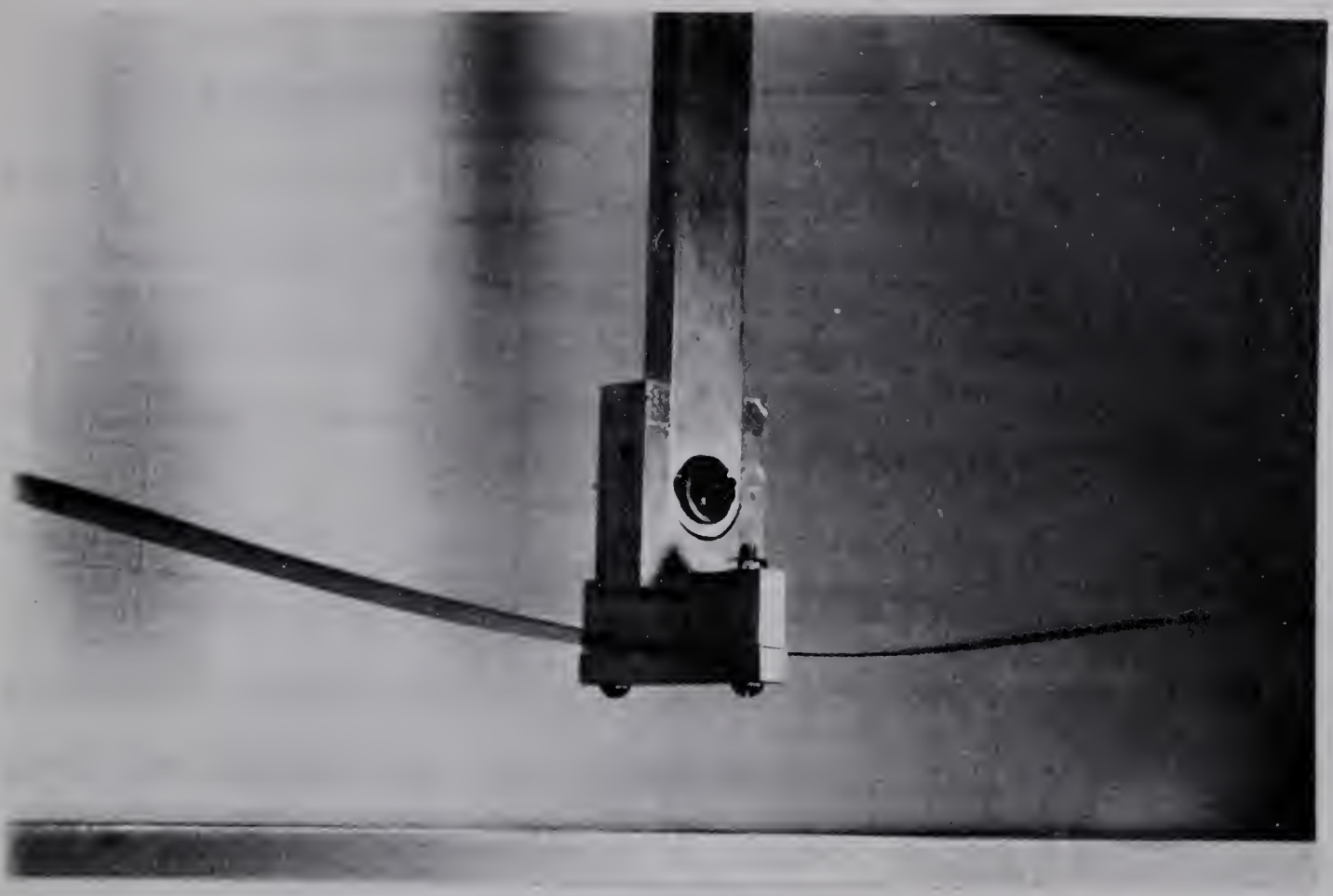

FIGURE 4.4 CENTRAL CLAMP.

FIGURE 4.5 DEFORMED ARCH RETAINING SYMMETRY.

Pertinent data for the eleven arches which were tested experimentally is given in Table 4.1, and, for the sake of convenience, each specimen has been given an identifying number.

The arches selected covered a wide range of arch geometry and weight to upper buckling load ratio.

4.3 Experimental Procedure

With a test-piece firmly located in the apparatus, the weight required to balance the scale was noted. The loading bar was lowered until the loading head just touched the arch. The head was securely fixed to the arch center to keep the tangent at that point horizontal. The arch was then deflected incrementally, and for each setting the balancing weight registered on the scale arm was noted. Thus with the scale adjusted so that the scale pan was again held at the original height, a situation was obtained whereby a measured central load induced the arch to deflect a given distance. The zero reading, i.e., the weight required to balance without any deflection was again noted, and if it differed from the initial value, the whole set of readings was discarded. The process was repeated three to four times for each specimen and the average readings were plotted.

Table 4.1

Dimensions of Test Specimens

Identifying Number	Semi-angle Ω	Radius of Curvature R_o in inches	Thickness t in inches	Non-dimensional parameter $\lambda = R_o\Omega^2/t$
S1	10°	82.67	0.015	166.77
S2	10°	69.08	0.015	139.36
S3	10°	82.67	0.026	96.86
S4	10°	69.08	0.026	80.94
S5	15°	55.47	0.015	251.76
S6	15°	46.35	0.015	210.38
S7	15°	55.47	0.026	146.22
S8	15°	46.35	0.026	122.18
S9	20°	41.97	0.015	338.70
S10	20°	41.97	0.026	196.71
S11	20°	35.07	0.026	164.37

Width = 0.75 inch

Modulus of Elasticity = 29.9×10^6 psi

Material: Banding Steel

CHAPTER V

RESULTS AND CONCLUSIONS

5.1 Load-Deflection Curves

The load-deflection curves for the symmetrical deformation of specimens S1 - S11, obtained by the application of the elastica approach neglecting arch weight, i.e., by the solution of differential equation as outlined in (1), as well as the ones obtained by considering the effects of arch weight, i.e., by the solution of differential equation 2.8, are presented in Figures 5.1 to 5.11. Experimental results obtained by the deflection controlled procedure explained in Chapter IV are included for each specimen. In all cases, results obtained from the Gjelsvik and Bodner (3) and the Schreyer and Masur (8) theories are given for comparison. Whereas the experimental results have a large discrepancy in most of the cases from the previous work of Gjelsvik and Bodner, Schreyer and Masur, and Kennedy, they are in good agreement with the present theoretical analysis.

5.2 Buckling Loads

Upper and Lower buckling loads for specimens S1 - S11 obtained from the respective Load-Deflection curve are given in Table 5.1. Following notations are used

$\overline{P}_{UN}$ = Non-dimensional Upper Buckling Load

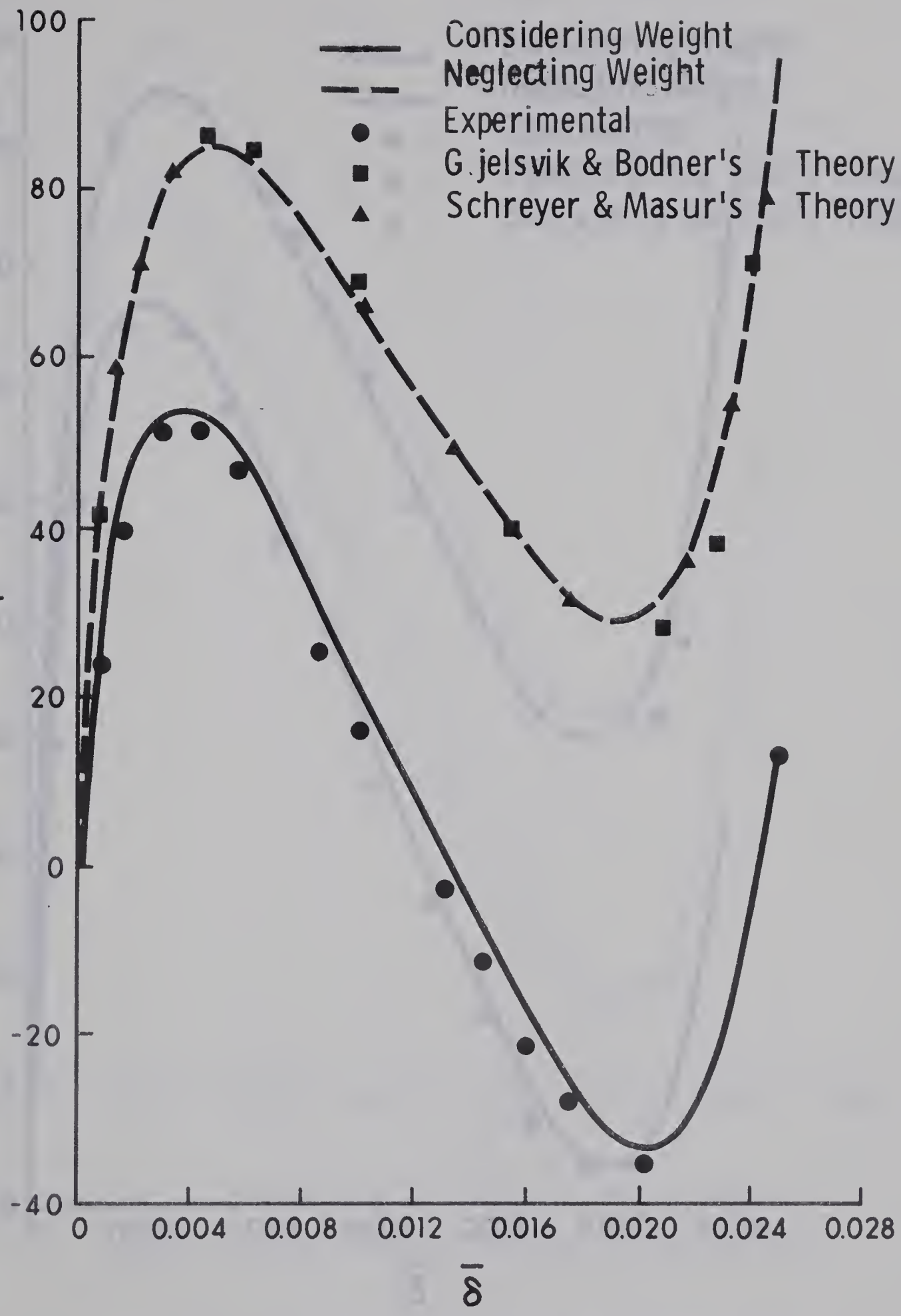

FIGURE 5.1 LOAD-DEFLECTION CURVES FOR SPECIMEN S1

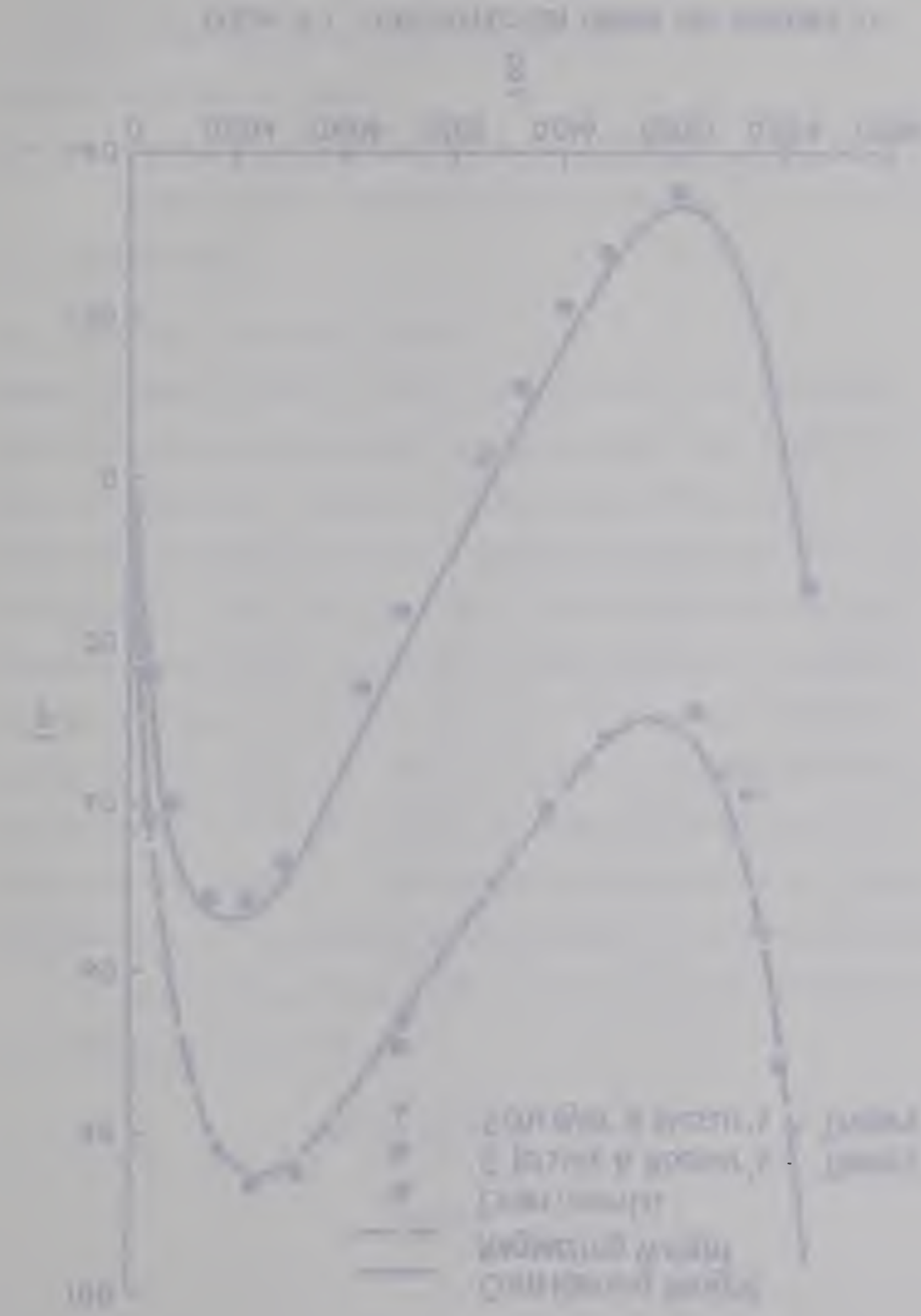

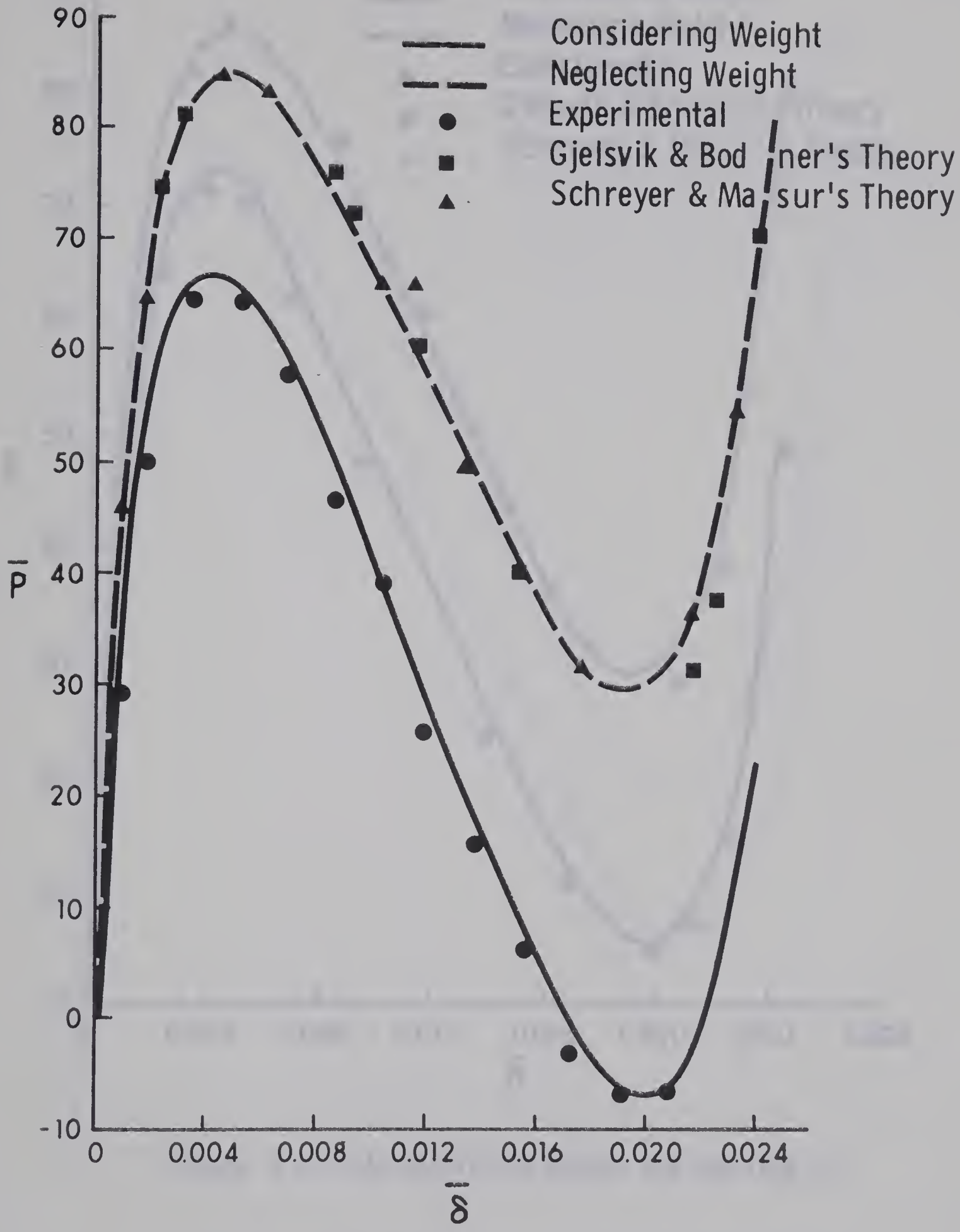

FIGURE 5.2 LOAD-DEFLECTION CURVES FOR SPECIMEN S2

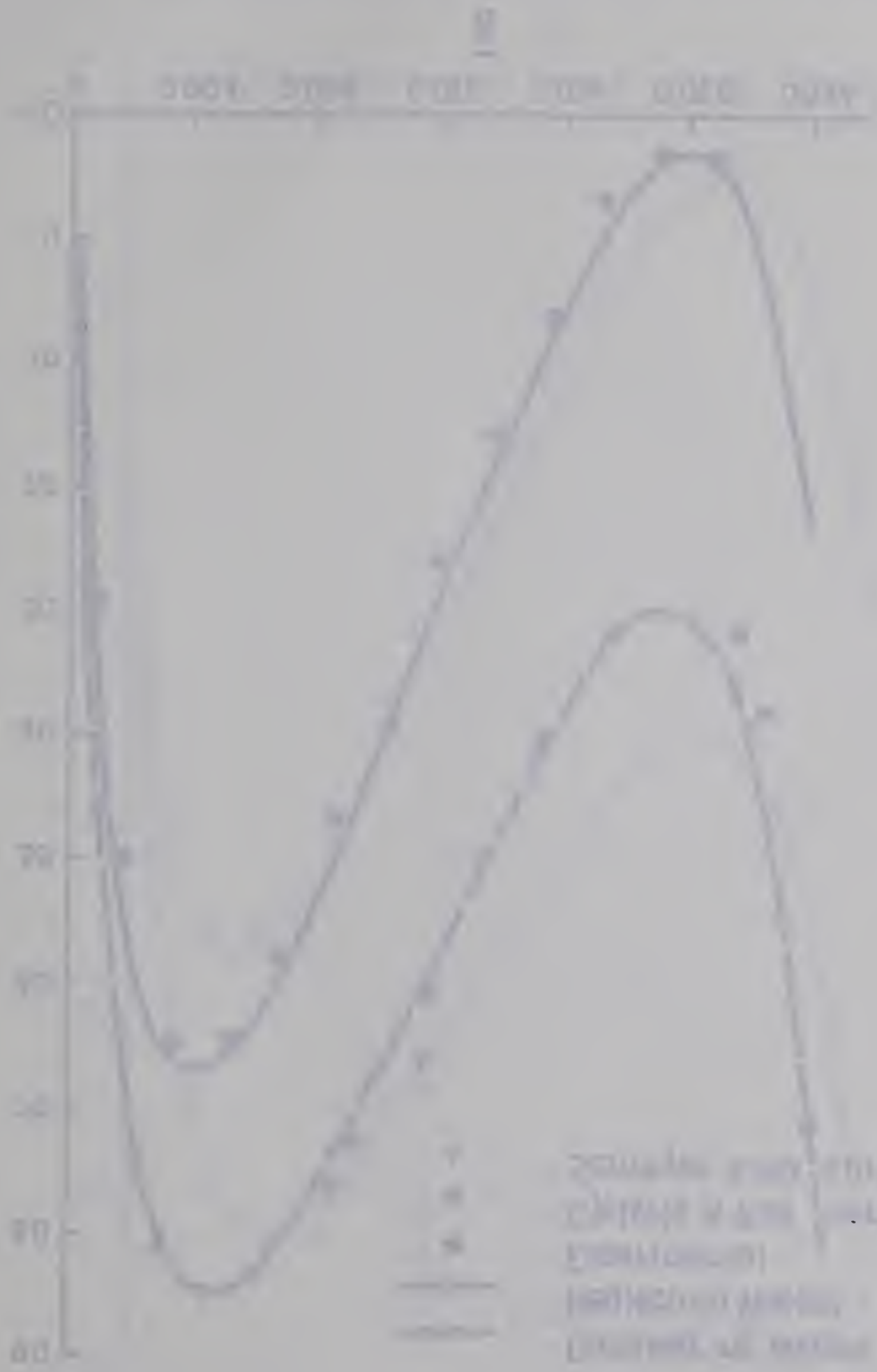

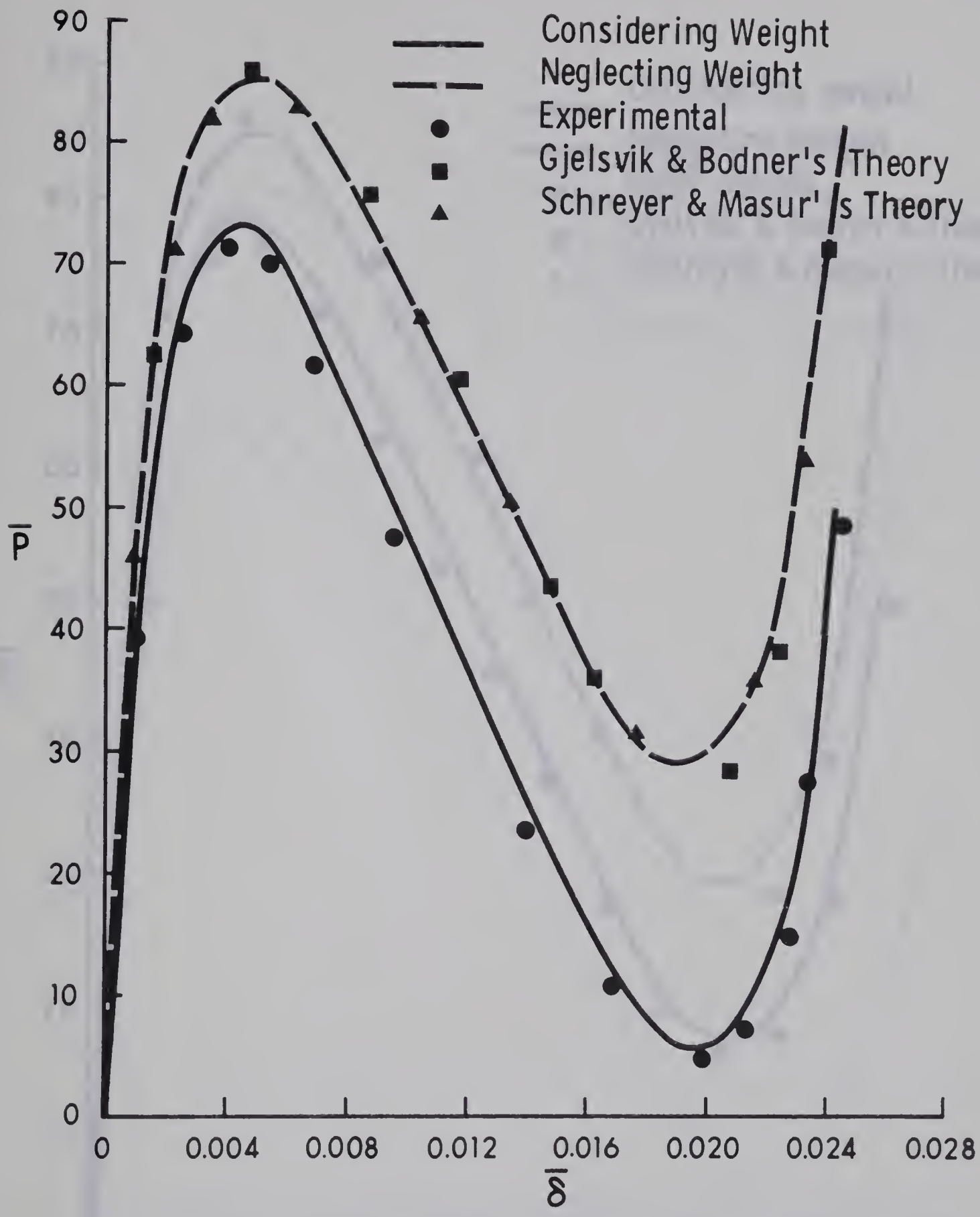

FIGURE 5.3 LOAD-DEFLECTION CURVES FOR SPECIMEN S3

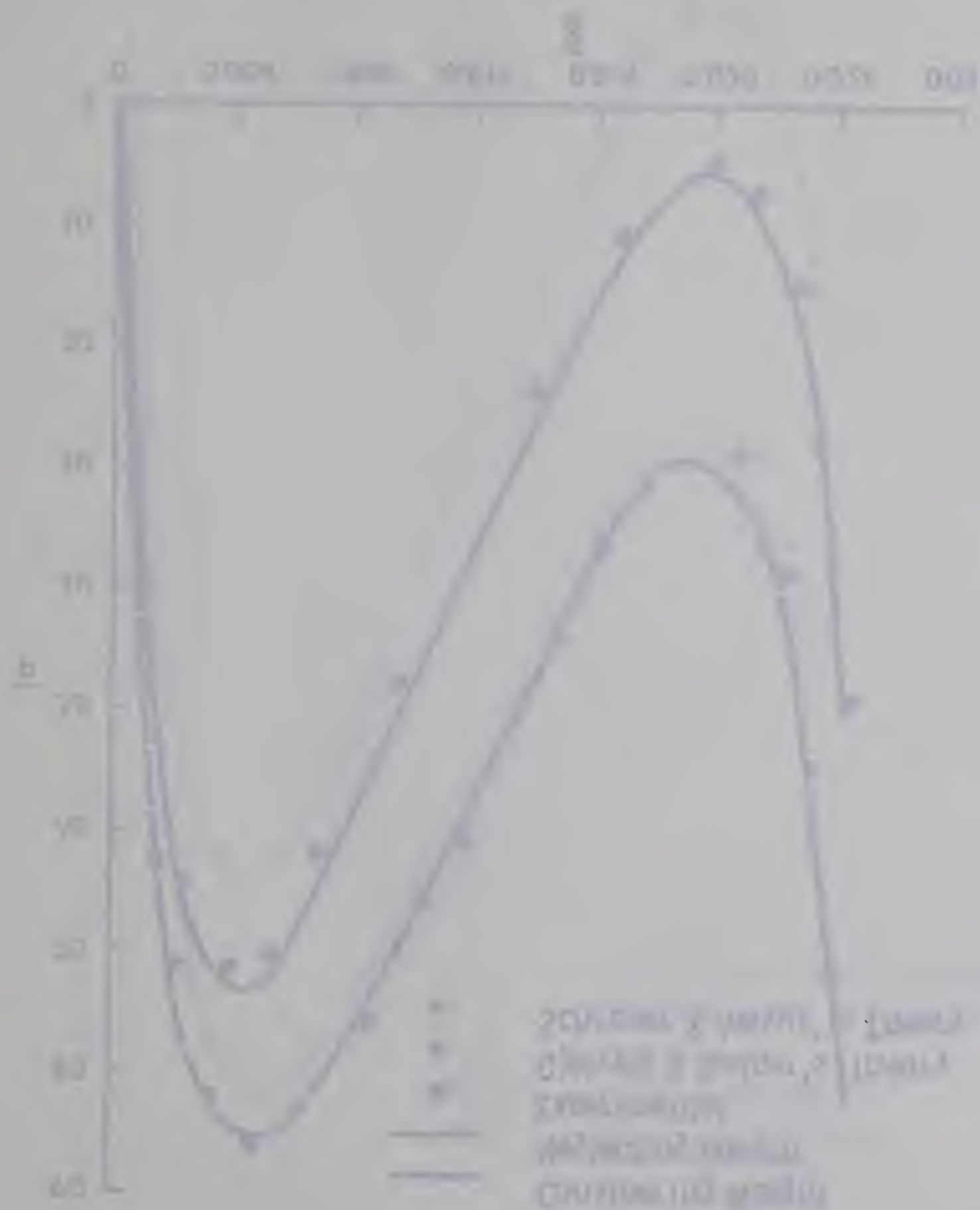

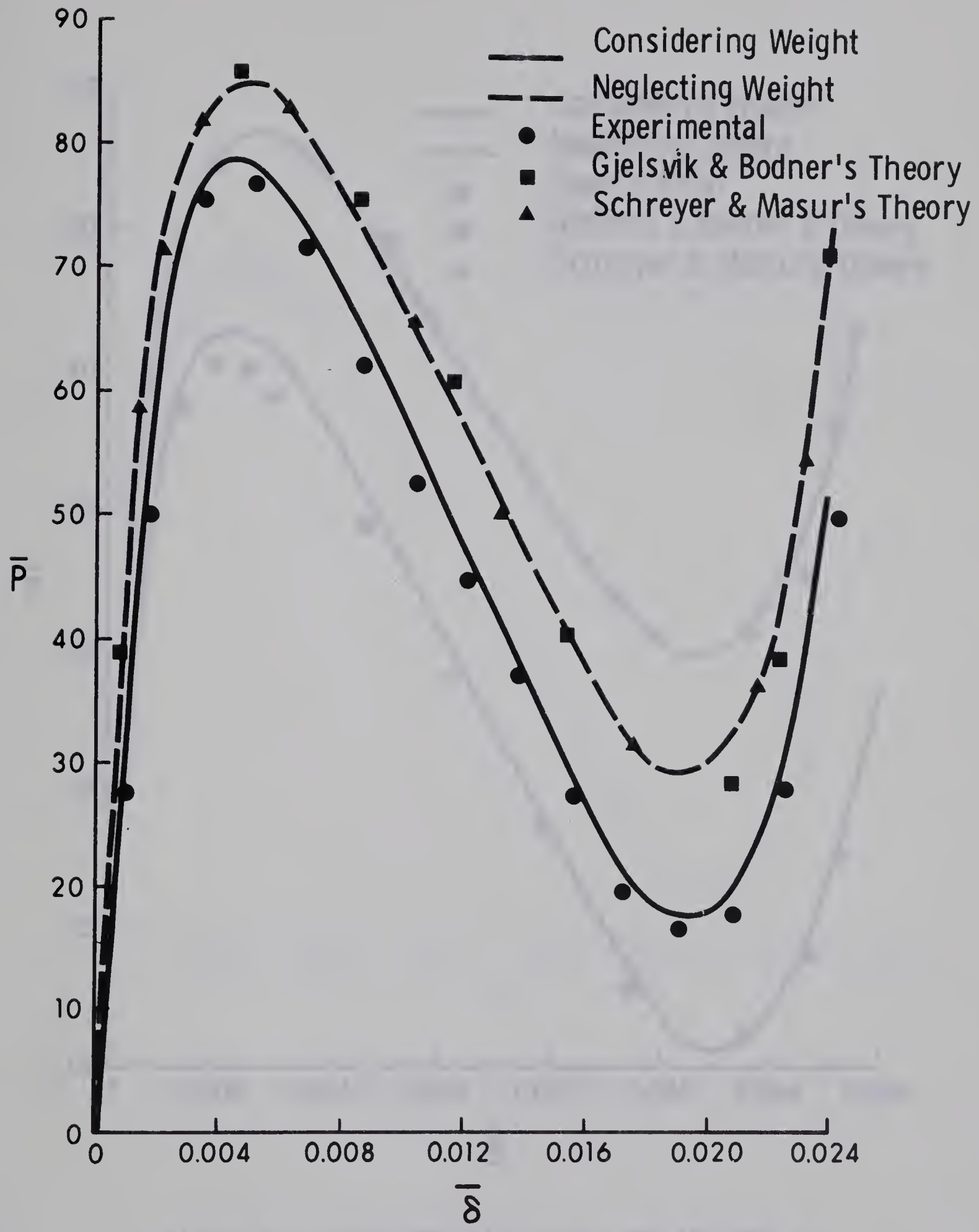

FIGURE 5.4 LOAD-DEFLECTION CURVES FOR SPECIMEN S4

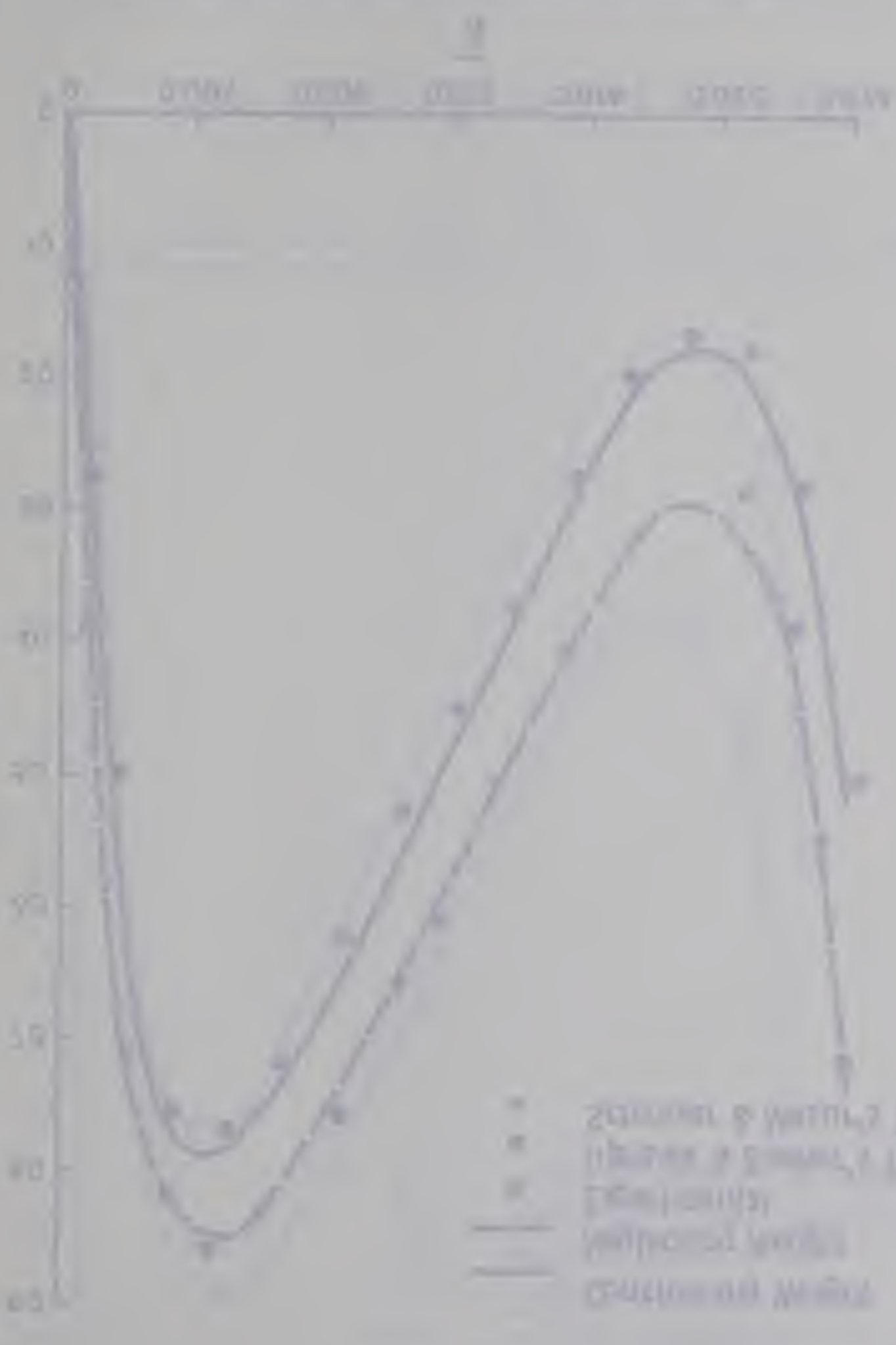

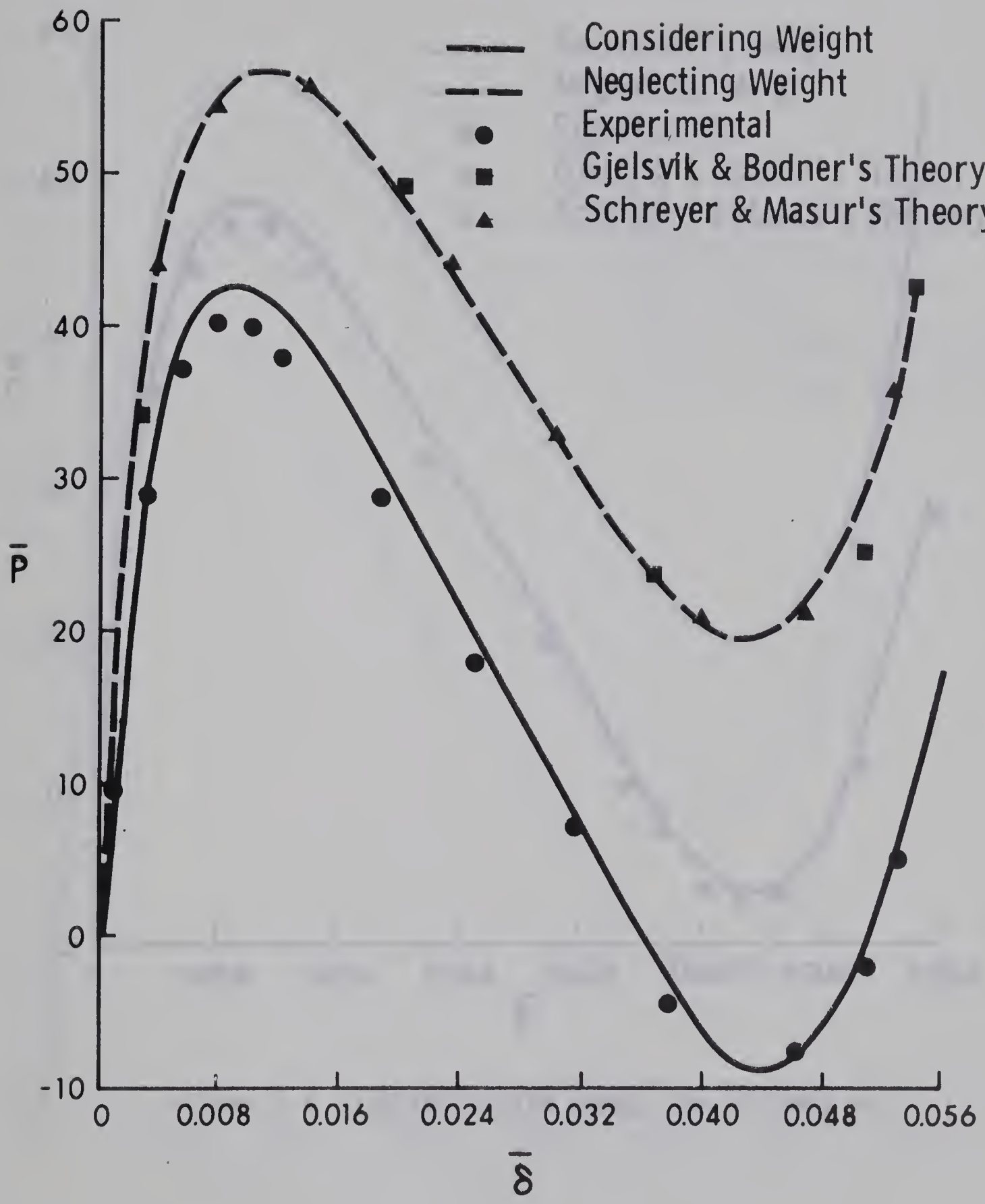

FIGURE 5.5 LOAD-DEFLECTION CURVES FOR SPECIMEN S5

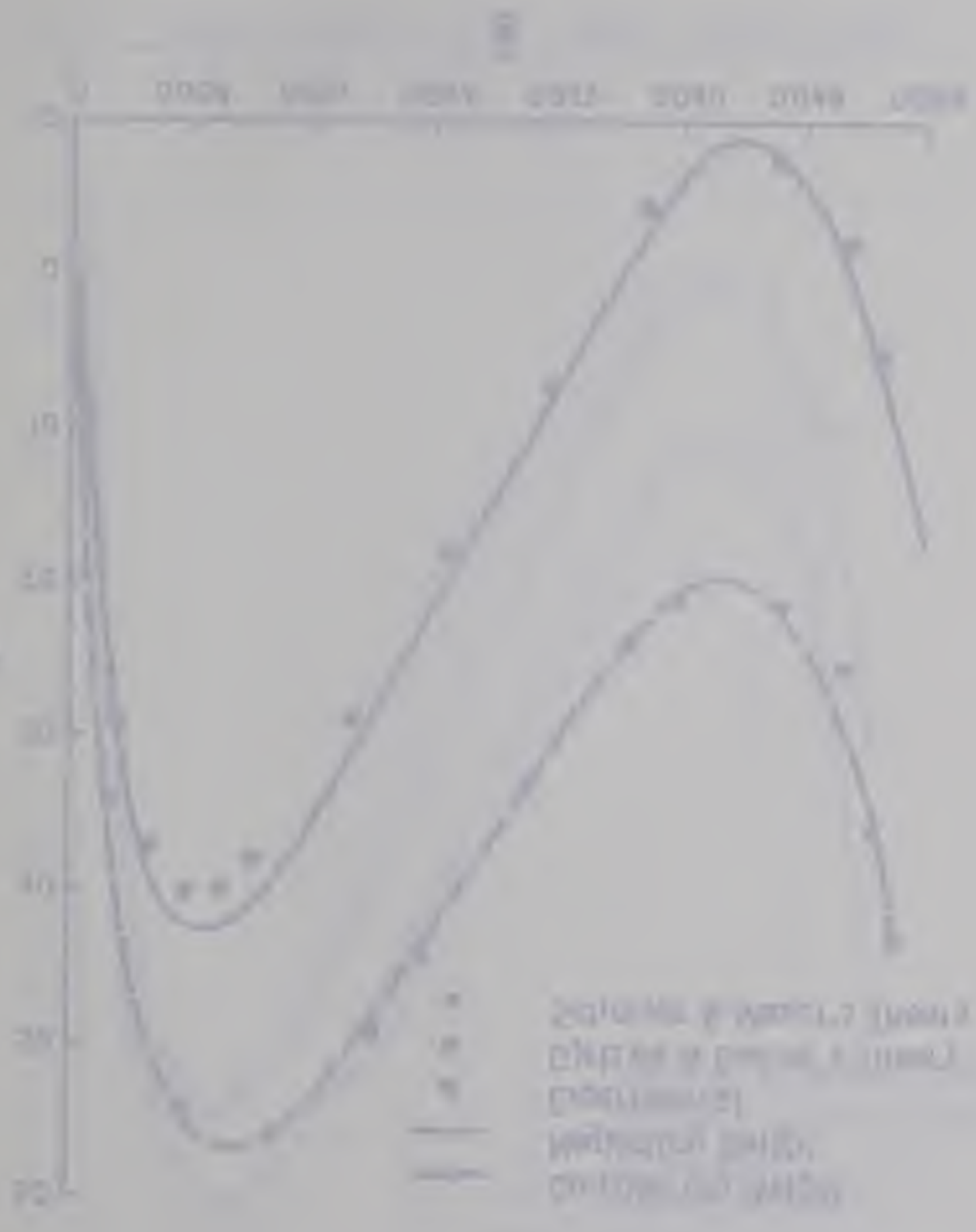

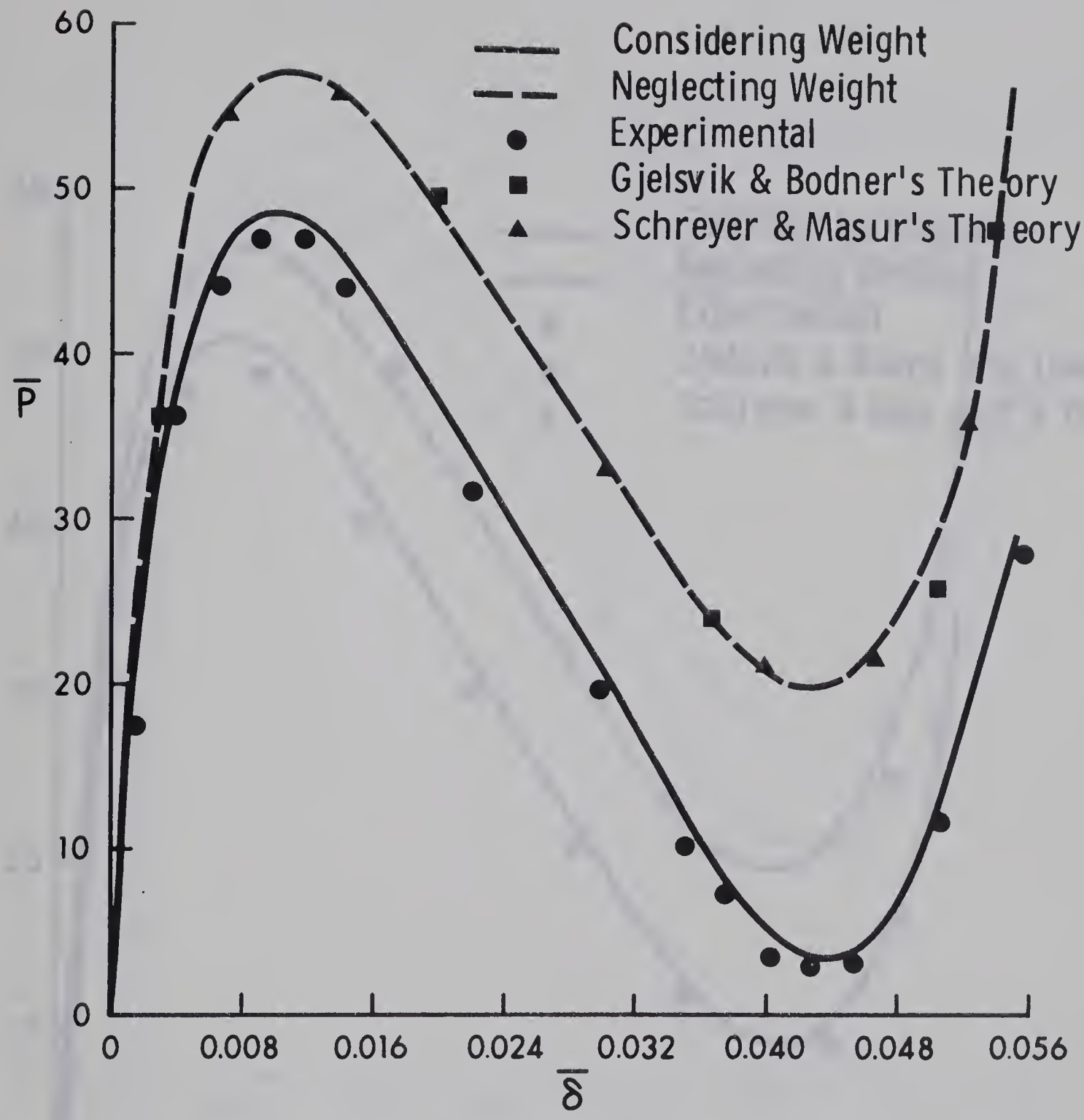

FIGURE 5.6 LOAD-DEFLECTION CURVES FOR SPECIMEN S6

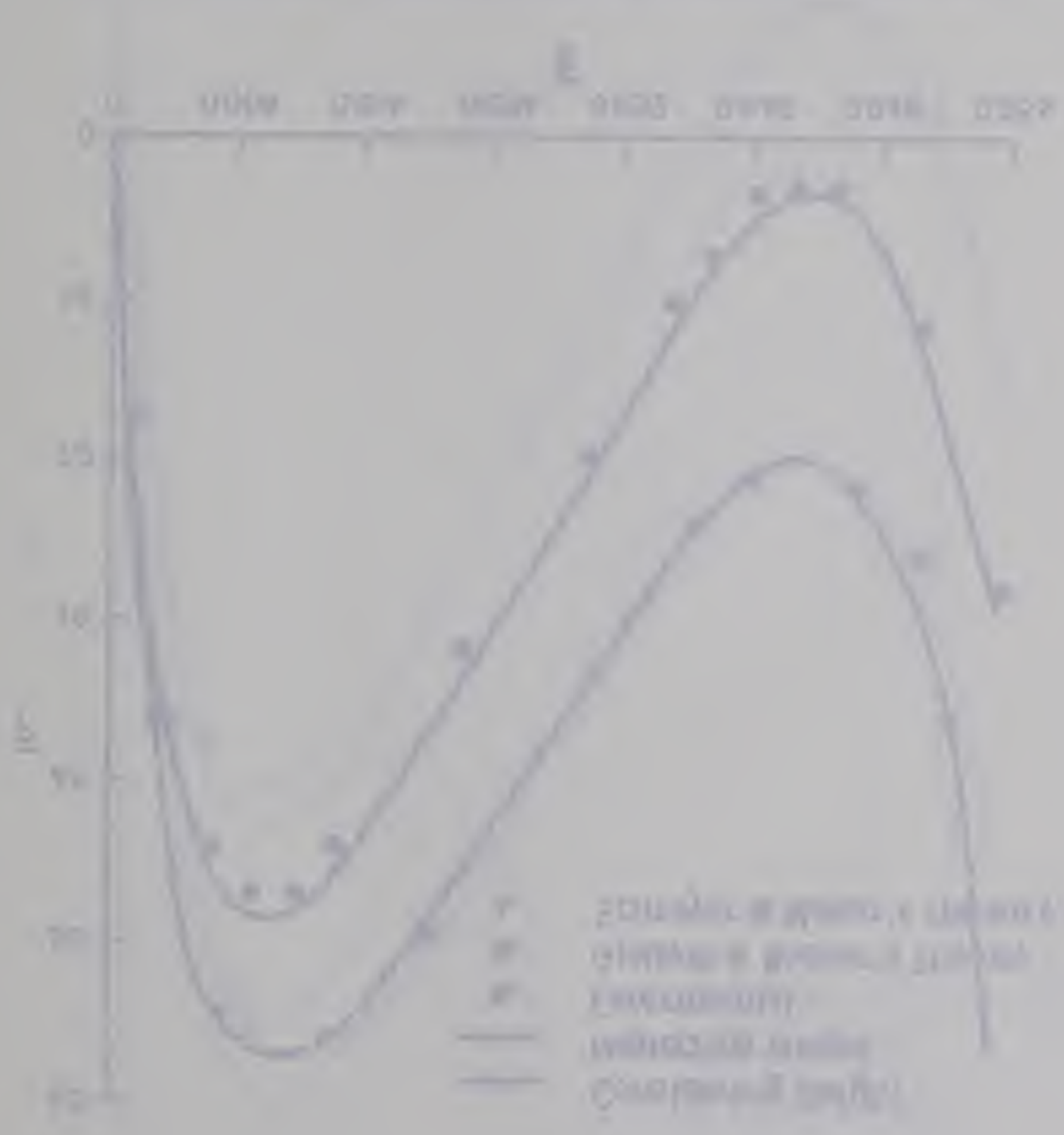

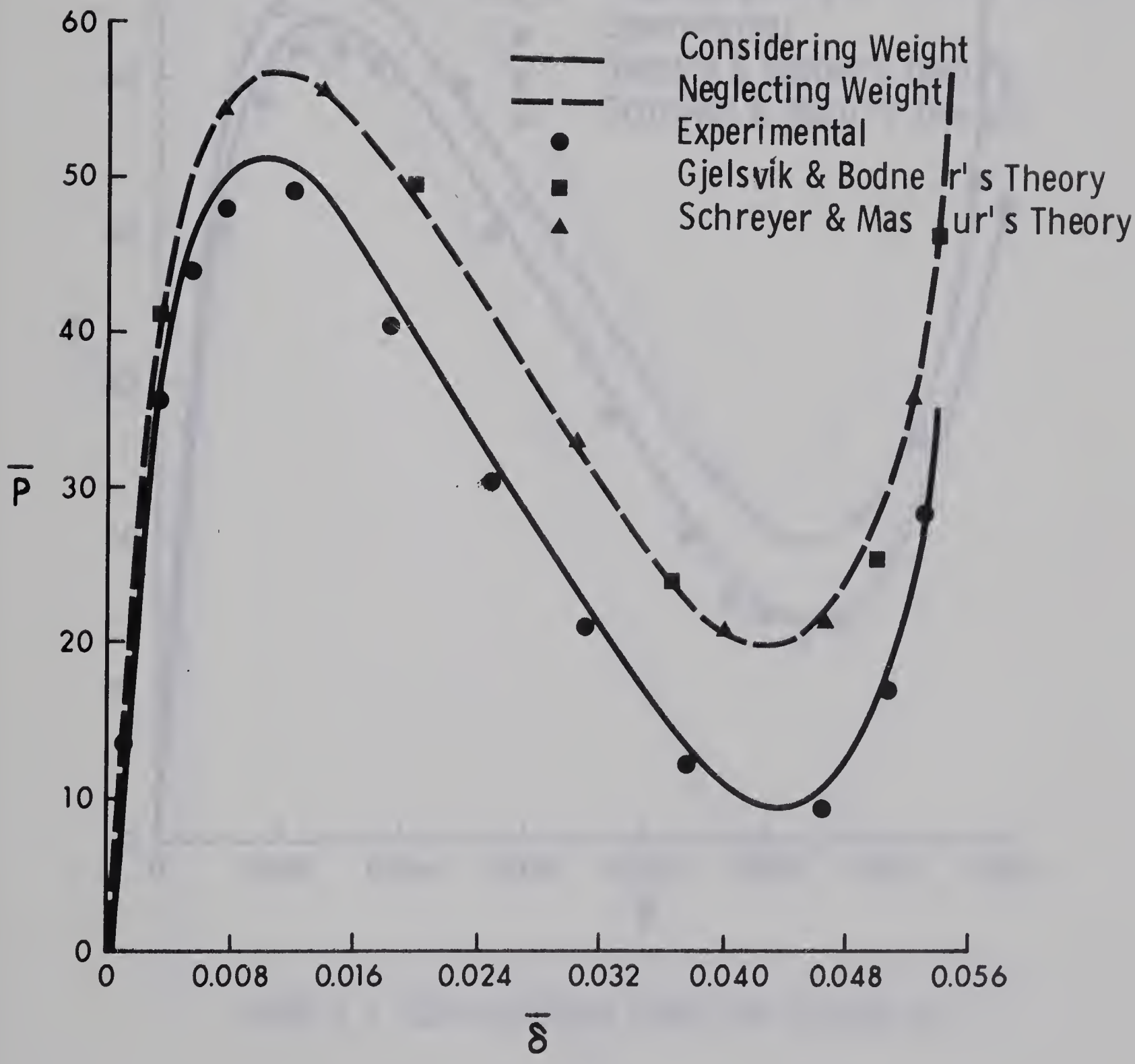

FIGURE 5.7 LOAD-DEFLECTION CURVES FOR SPECIMEN S7

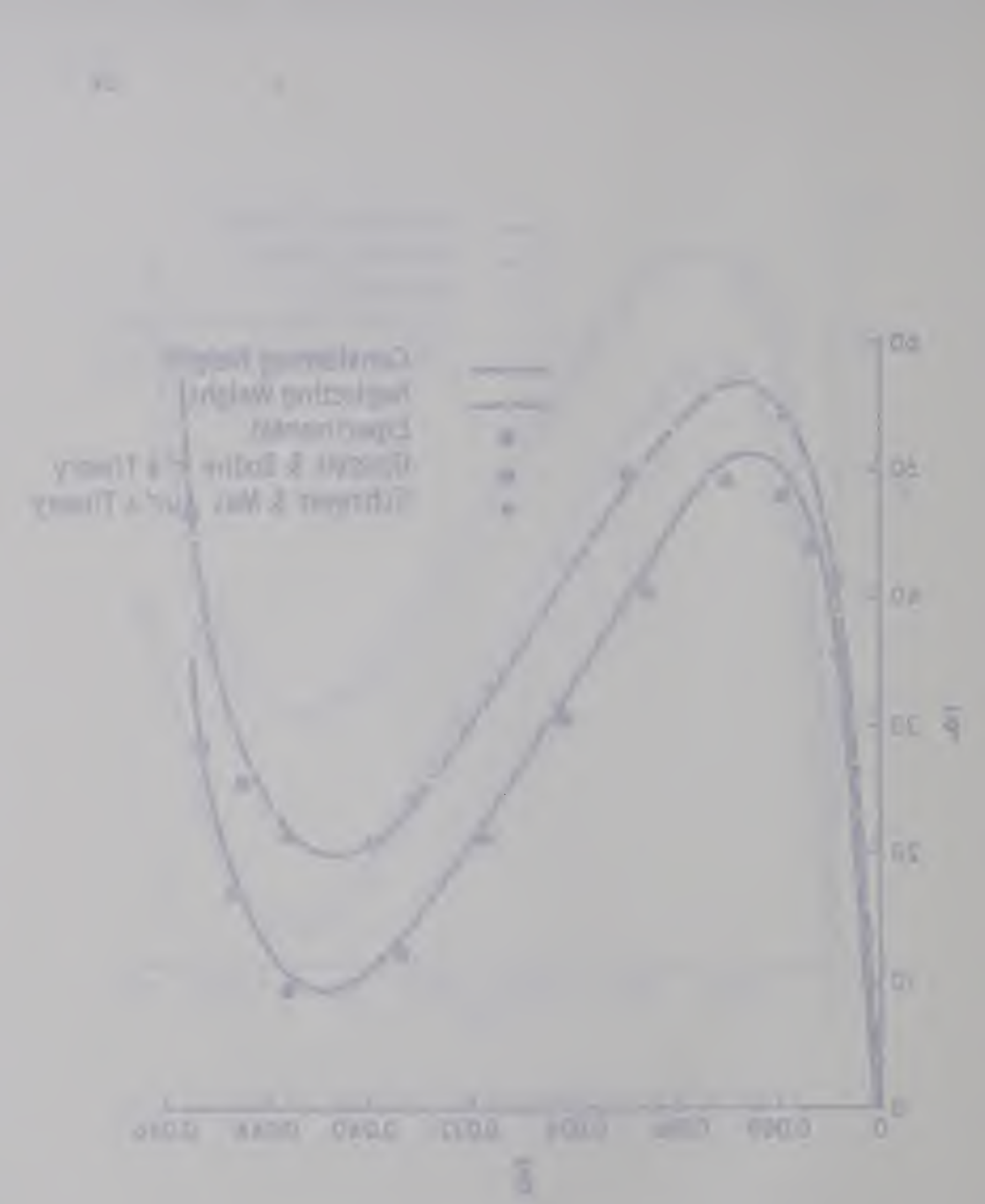

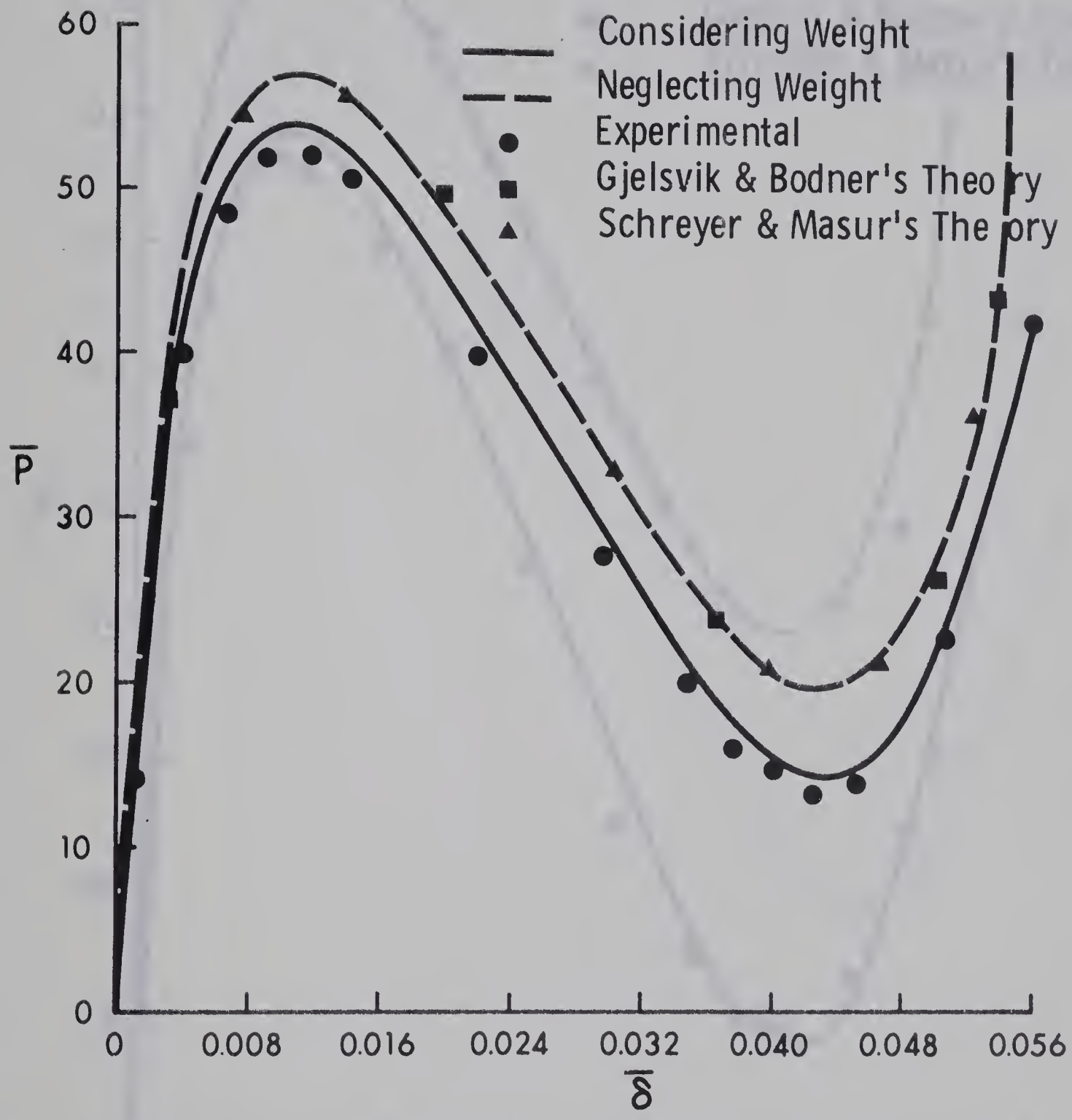

FIGURE 5.8 LOAD-DEFLECTION CURVES FOR SPECIMEN S8

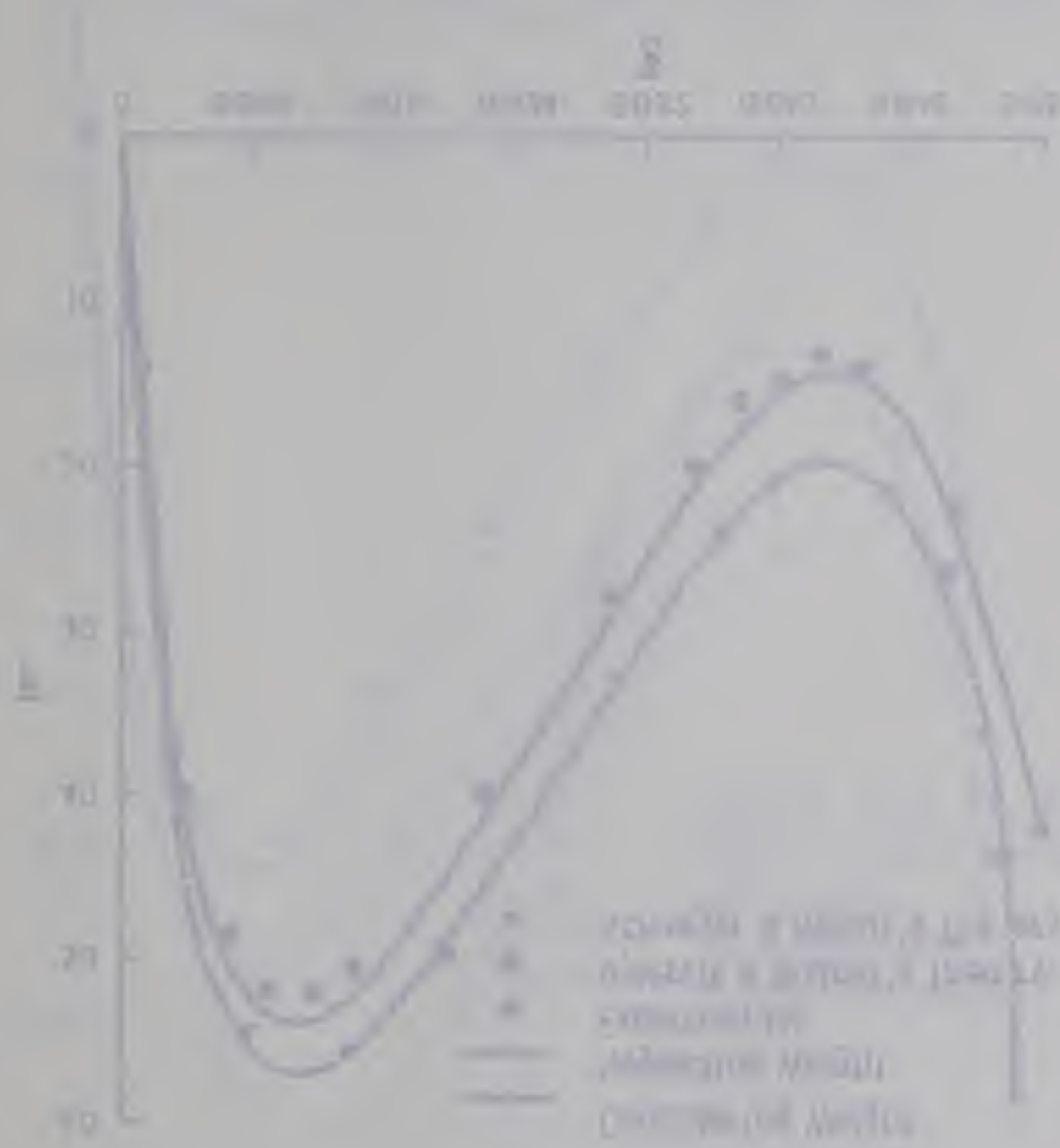

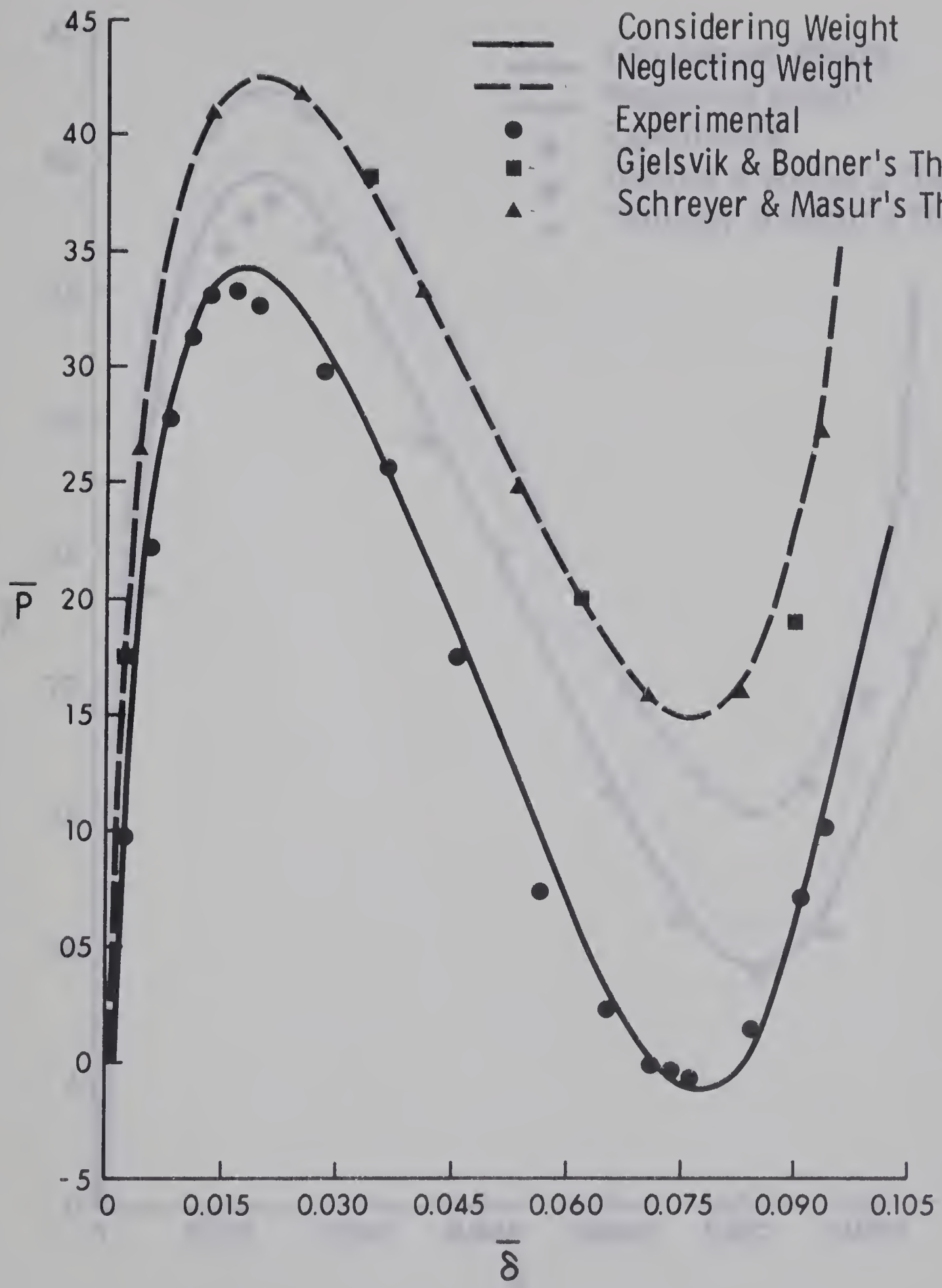

FIGURE 5.9 LOAD-DEFLECTION CURVES FOR SPECIMEN S9

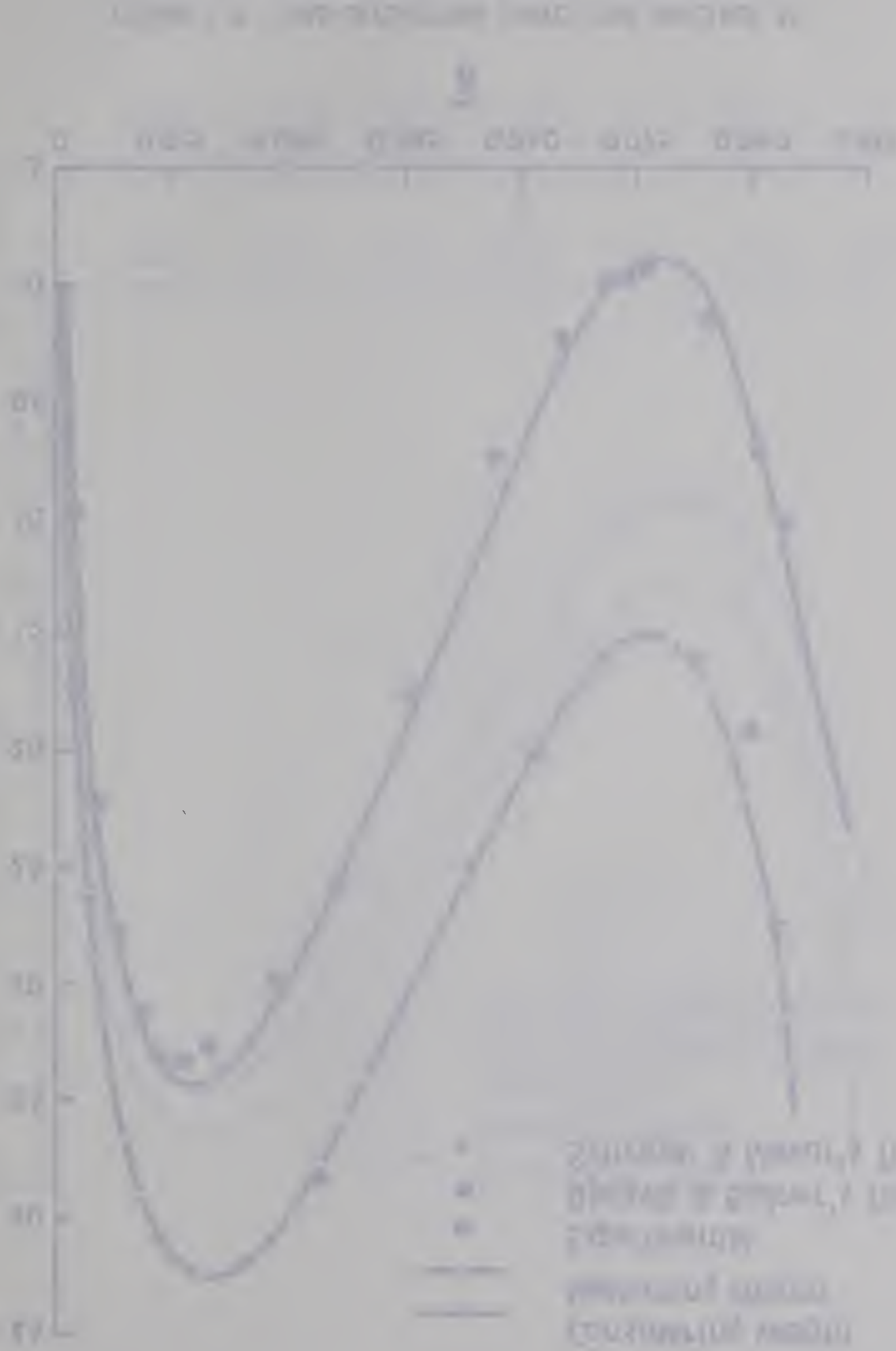

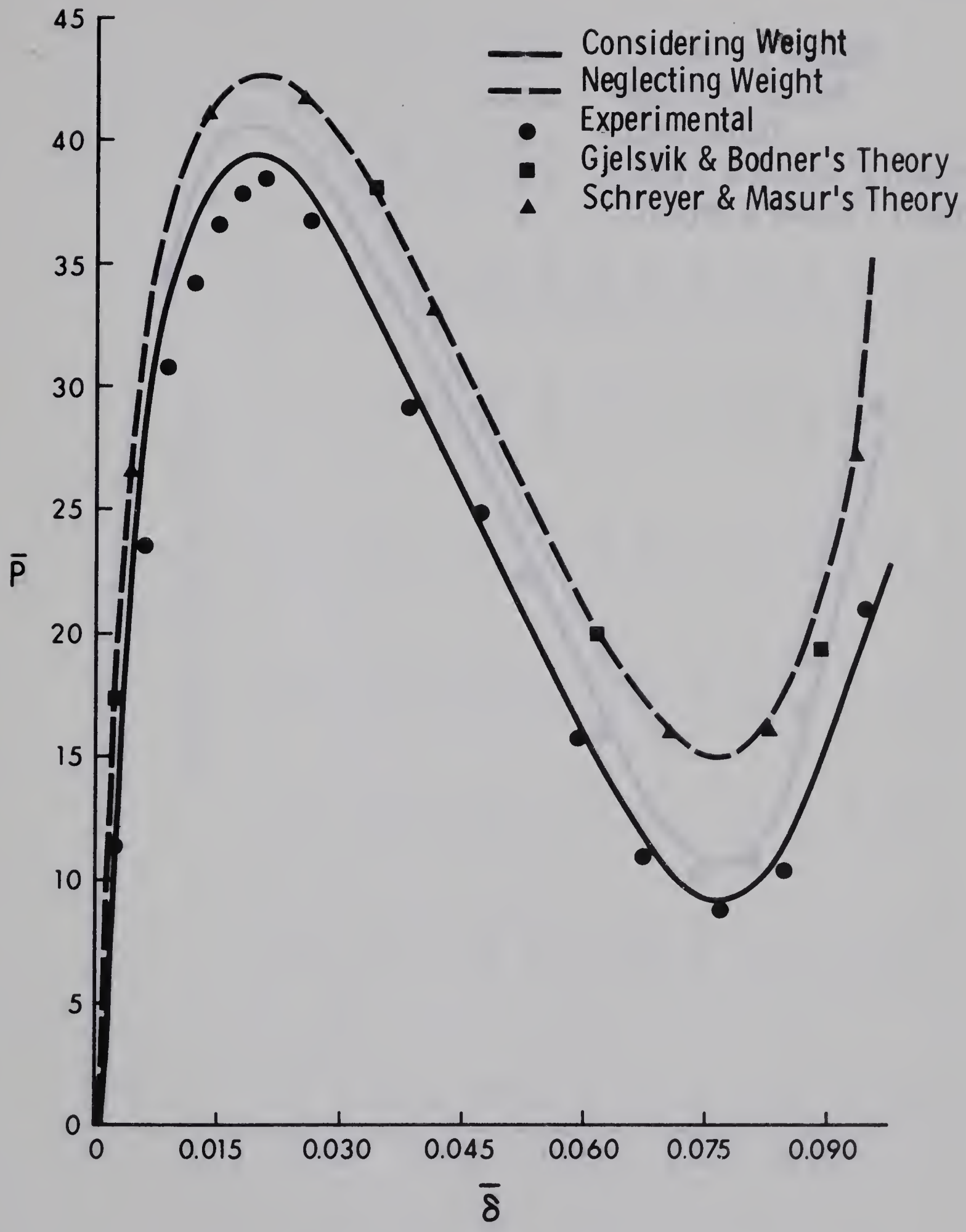

FIGURE 5.10 LOAD-DEFLECTION CURVES FOR SPECIMEN S10

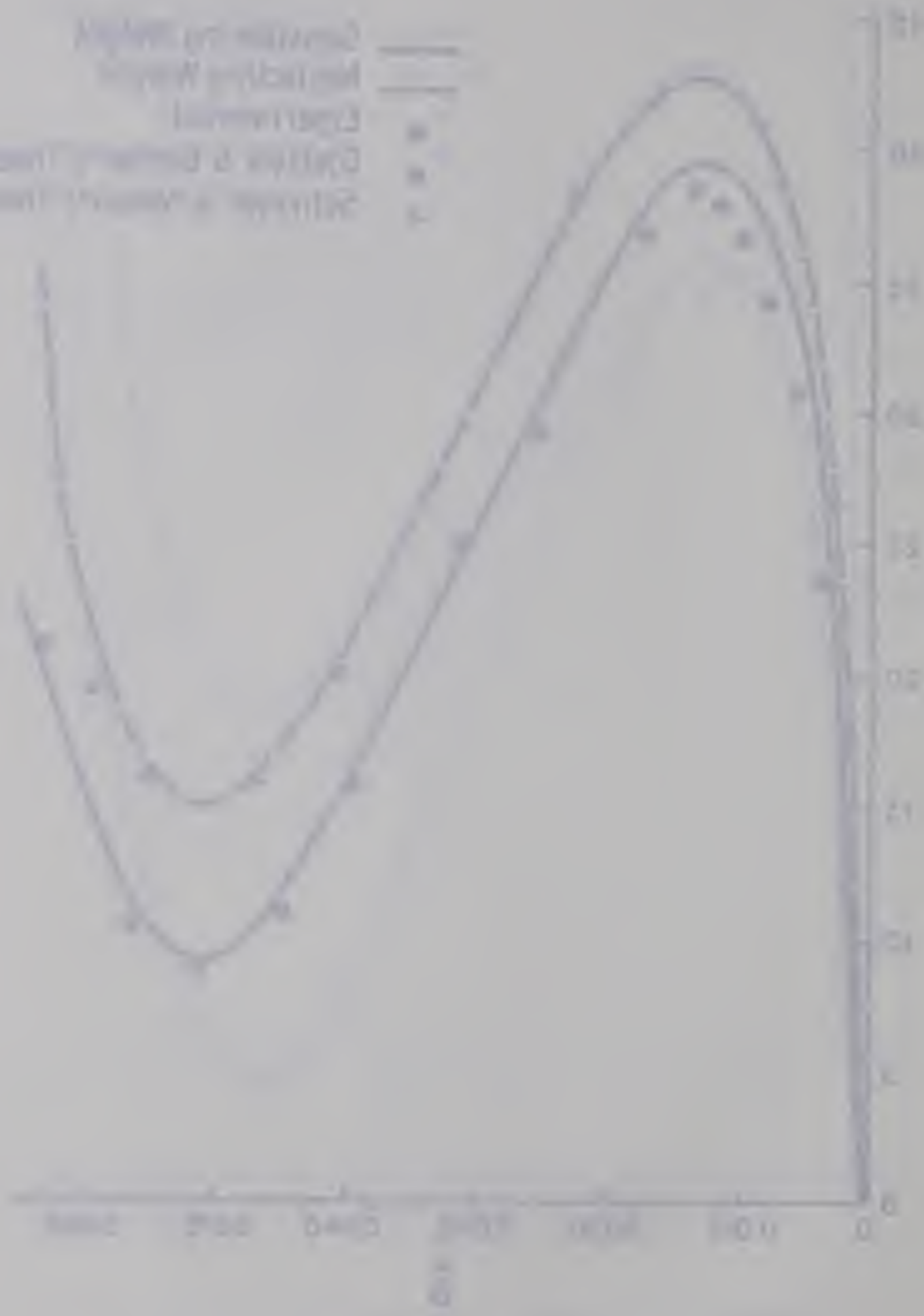

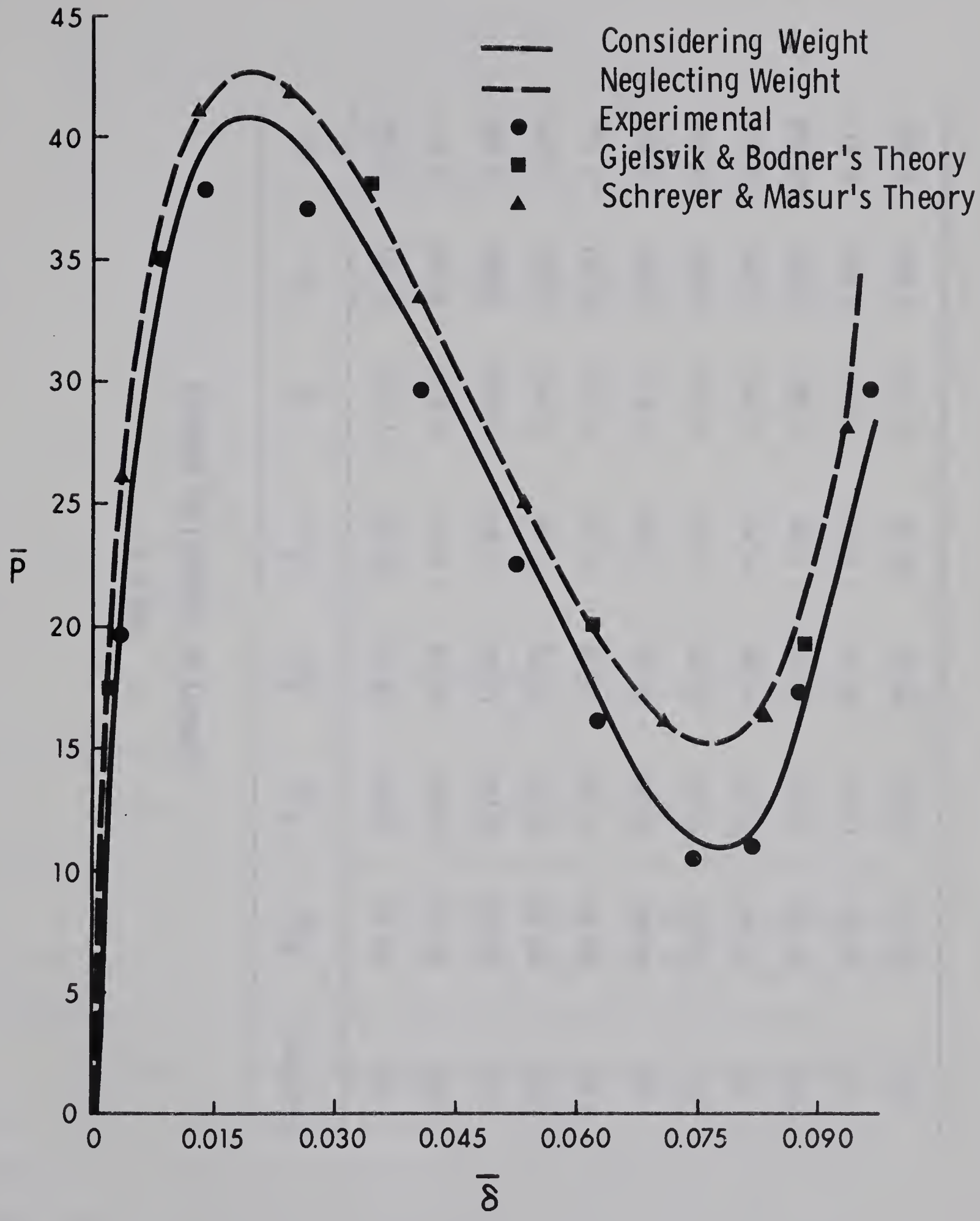

FIGURE 5.11 LOAD-DEFLECTION CURVES FOR SPECIMEN S11

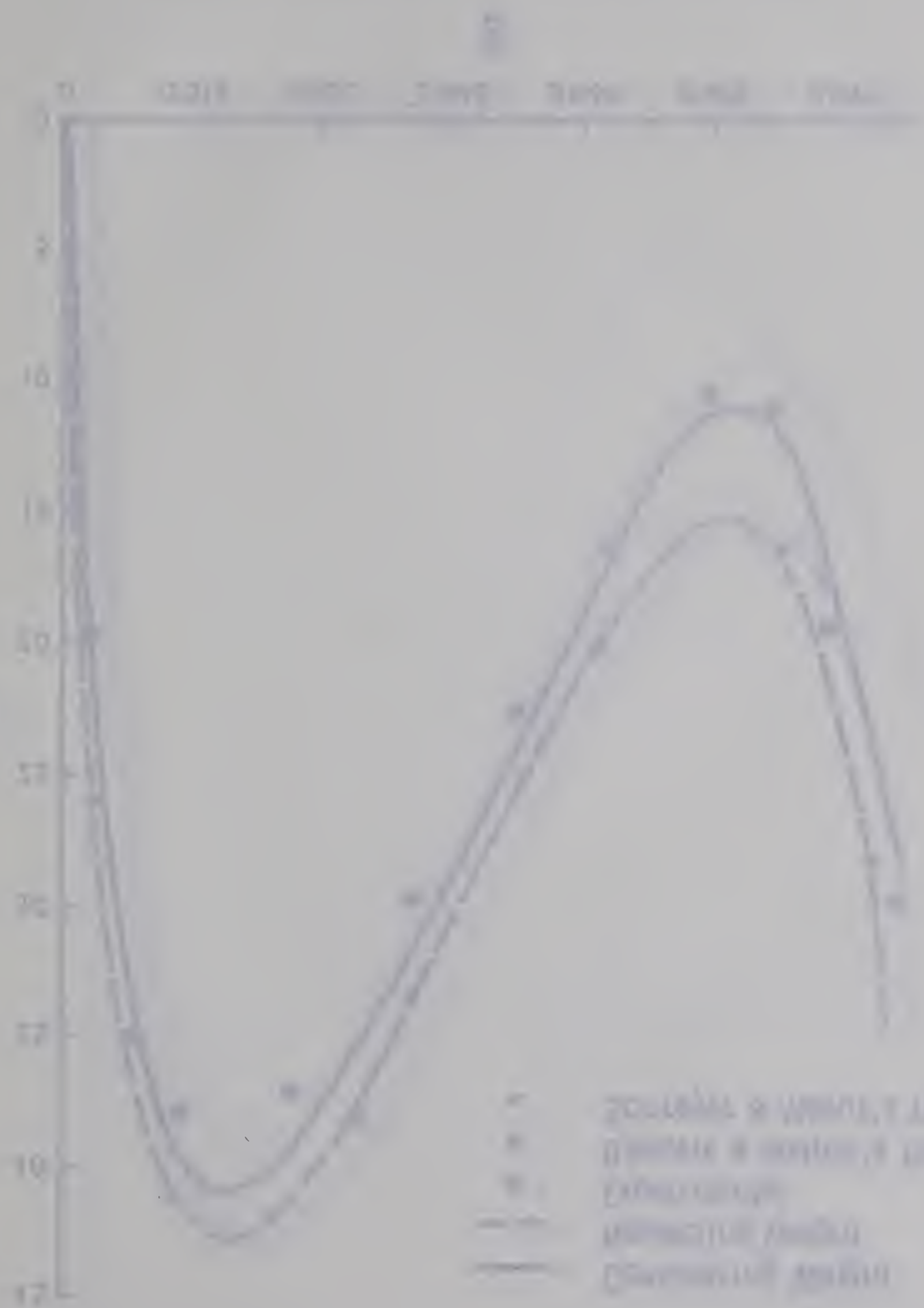

TABLE 5.1

SUMMARY OF THEORETICAL RESULTS

Specimen	$\overline{P}_{UN}$	$\overline{P}_{LN}$	$\overline{P}_{UC}$	$\overline{P}_{LC}$	ρ_W	ρ_U	ρ_L
S1	85.00	29.50	54.50	-33.50	1.126	0.641	-0.394
S2	85.00	29.50	66.75	- 6.75	0.657	0.785	-0.070
S3	85.00	29.50	73.00	5.50	0.388	0.858	0.065
S4	85.00	29.50	78.75	17.50	0.266	0.926	0.205
S5	56.60	19.92	42.72	- 8.52	0.766	0.754	-0.150
S6	56.60	19.92	48.48	3.60	0.447	0.856	0.063
S7	56.60	19.92	51.40	9.20	0.264	0.908	0.162
S8	56.60	19.92	54.00	14.40	0.154	0.954	0.254
S9	42.56	15.10	34.37	- 1.05	0.589	0.807	-0.024
S10	42.56	15.10	39.37	9.25	0.203	0.925	0.217
S11	42.56	15.10	40.87	10.75	0.118	0.960	0.252

$\overline{P}_{LN}$ = Non-dimensional Lower Buckling Load

$\overline{P}_{UC}$ = Non-dimensional Upper Buckling Load considering the effects of arch weight

$\overline{P}_{LC}$ = Non-dimensional Lower Buckling Load considering the effects of arch weight

ρ_W = Ratio of non-dimensional arch weight and Upper Buckling Load

$= \overline{\rho}/\overline{P}_{UN}$

ρ_U = Ratio of $\overline{P}_{UC}$ and $\overline{P}_{UN}$

$= \overline{P}_{UC}/\overline{P}_{UN}$

ρ_L = Ratio of $\overline{P}_{LC}$ and $\overline{P}_{UN}$

$= \overline{P}_{LC}/\overline{P}_{UN}$

ρ_U and ρ_L are plotted as functions of ρ_W in Figure 5.12.

5.3 Conclusions

1. Figures 5.1 - 5.11 show that the arch weight has a significant effect on the large deflections of thin arches under concentrated load.

2. There is a linear relationship between ρ_W and ρ_U and between ρ_W and ρ_L, as shown in Figure 5.12. Both upper and lower buckling loads decrease as the arch weight to upper buckling load ratio increases.

3. Keeping the semi-angle and stiffness of the arch constant, the arch weight to buckling load ratio will increase by increasing the span. Therefore, in the case of longer arches, arch weight will have a more significant effect on the buckling loads.

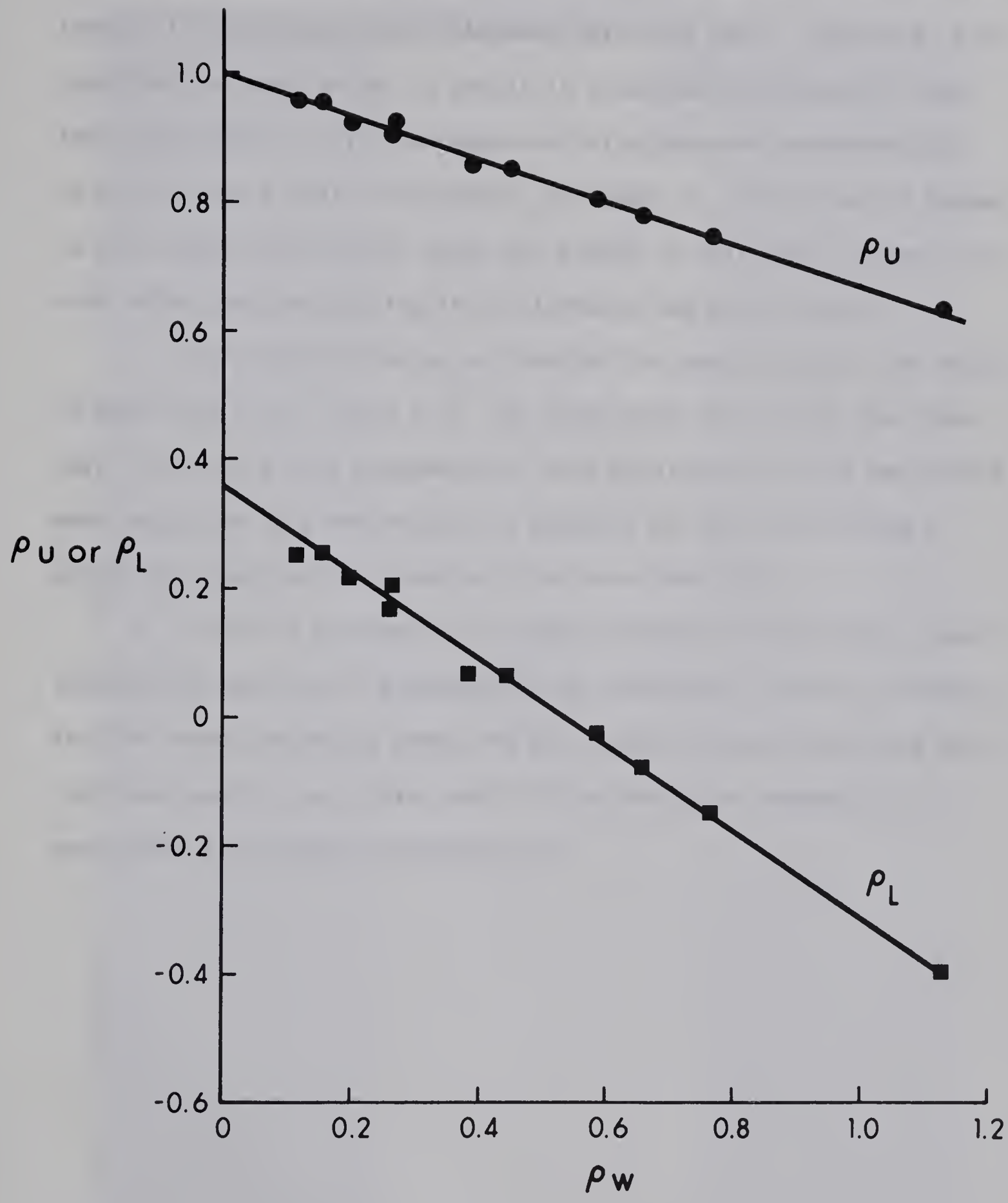

FIGURE 5.12 ρ_U AND ρ_L vs ρ_W

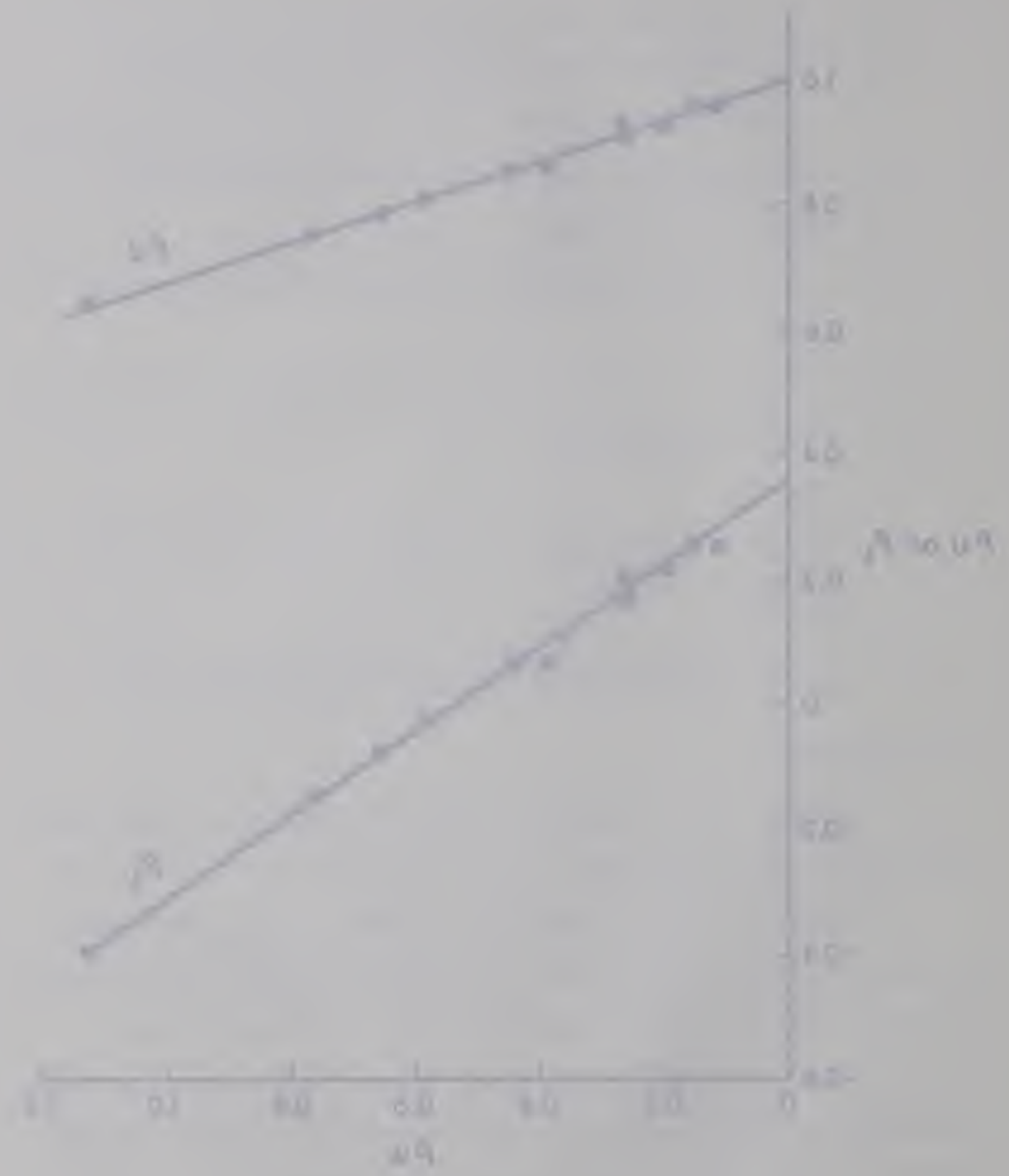

4. For specimens S1, S2, S5 and S9, the lower buckling load is lowered to the extent that it becomes less than zero. Therefore it is possible for these arches to remain in a buckled configuration under their own weight. This phenomenon was also observed experimentally. On being given a small disturbance, specimens S1, S2, S5 and S9 jumped to the symmetrical buckled shape and stayed in that form, Figure 5.13, even after the load causing the disturbance had been removed.

For any arch having arch weight to upper buckling load ratio of more than 0.53, Figure 5.12, the lower buckling load is less than zero. Therefore this phenomenon of arch buckling under its own weight when subjected to a disturbance is possible for any arch having a weight to upper buckling load ratio of more than 0.53.

5. Gjelsvik and Bodner (4) were successful in obtaining a good agreement between their experimental and theoretical results because for the arches tested by them the arch weight to upper buckling load ratio was small, i.e., less than 0.05 and hence the assumption of negligible arch weight was permissible.

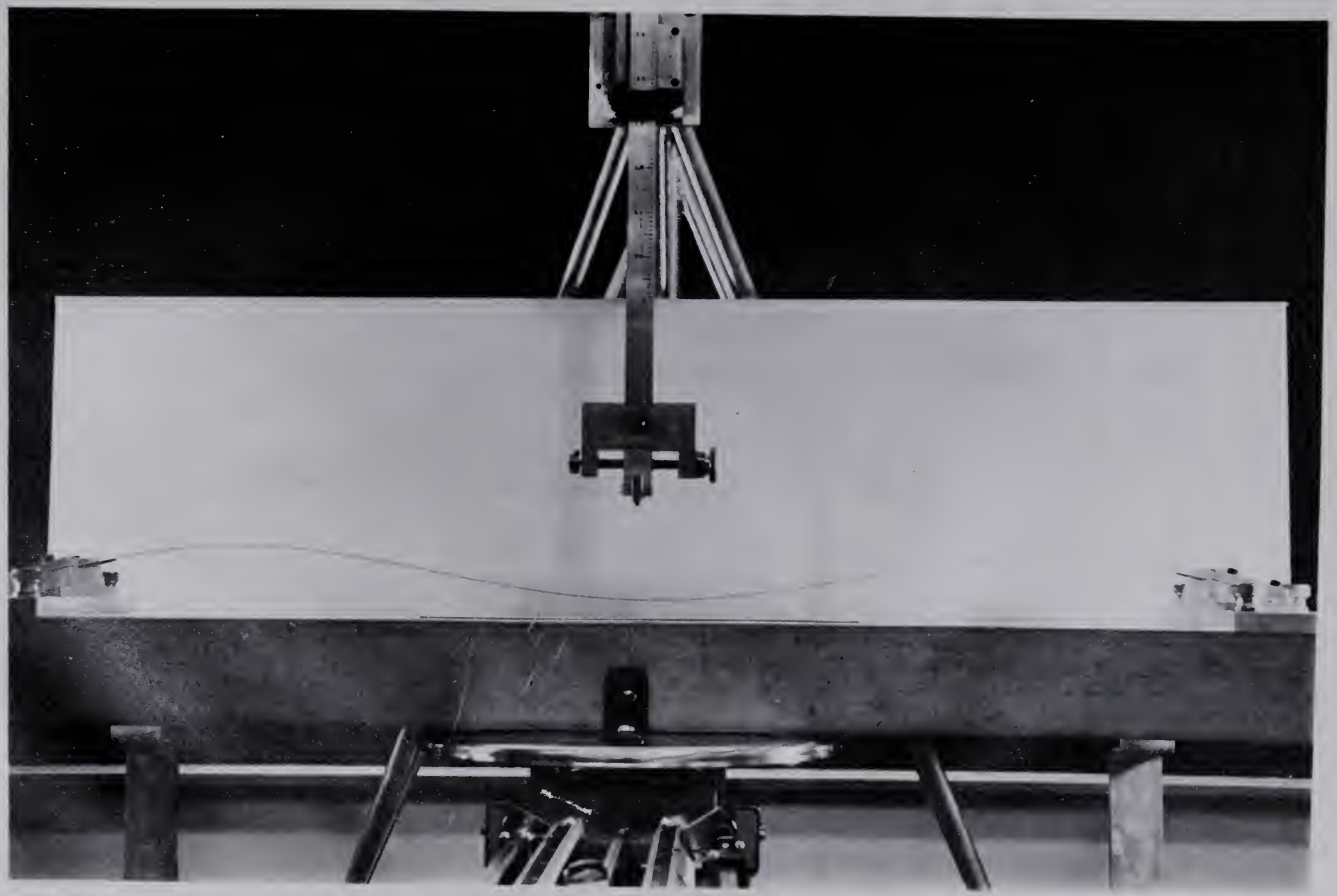

FIGURE 5.13 BUCKLED ARCH UNDER ITS OWN WEIGHT.

CHAPTER VI

FURTHER APPLICATIONS OF THE "SHOOTING" METHOD

1. The "shooting" method used by the author presents an elegant tool for the study of the large deflections of flexible elastic bars. A number of non-linear boundary value problems can be solved by this technique. For example, consider the large deflections of complete circular ring subjected to two equal and opposite, concentrated loads acting along a diameter. The complete ring is free to expand in the direction at right angles to the line of action of the loads. Therefore there will be no thrust N_o, Figure 2.2. The angle β will therefore be $\pi/2$. The Equation 2.8 for this case reduces to

$$\frac{d^2\phi}{d\bar{s}^2} + \bar{F} \sin(\phi - \frac{\pi}{2}) = 0 \qquad 6.1$$

neglecting effects due to ring weight.

Boundary conditions for this case are

$$\phi = 0 \quad \text{at} \quad \bar{s} = 0$$

$$\phi = \frac{\pi}{2} \quad \text{at} \quad \bar{s} = \frac{\pi}{2} \qquad 6.2$$

In this case the unknown initial value is $\frac{d\phi}{d\bar{s}}$ only. Following the same procedure as before the complete load deflection curve is obtained, Figure 6.1. For comparison, results obtained by Timeshenko and Gere (10) are also given in Figure 6.1.

2. With suitable modifications in boundary conditions, the method used in this thesis can also be applied to solve symmetrical deflections of pinned ends arches under concentrated radial load at the point of symmetry. Conditions 2.9 and 2.11 remain unchanged. Since there is no moment at the pinned ends, boundary condition 2.10 must be replaced by

$$\frac{d\phi}{d\bar{s}} = \frac{d\phi_o}{d\bar{s}} = 1 \quad \text{at} \quad \bar{s} = \Omega \qquad 6.3$$

3. Arches considered in this thesis were only 0.75 inch wide. The present work can be extended to cover wider arches and possibly cylindrical shells taking anticlastic deformation into account.

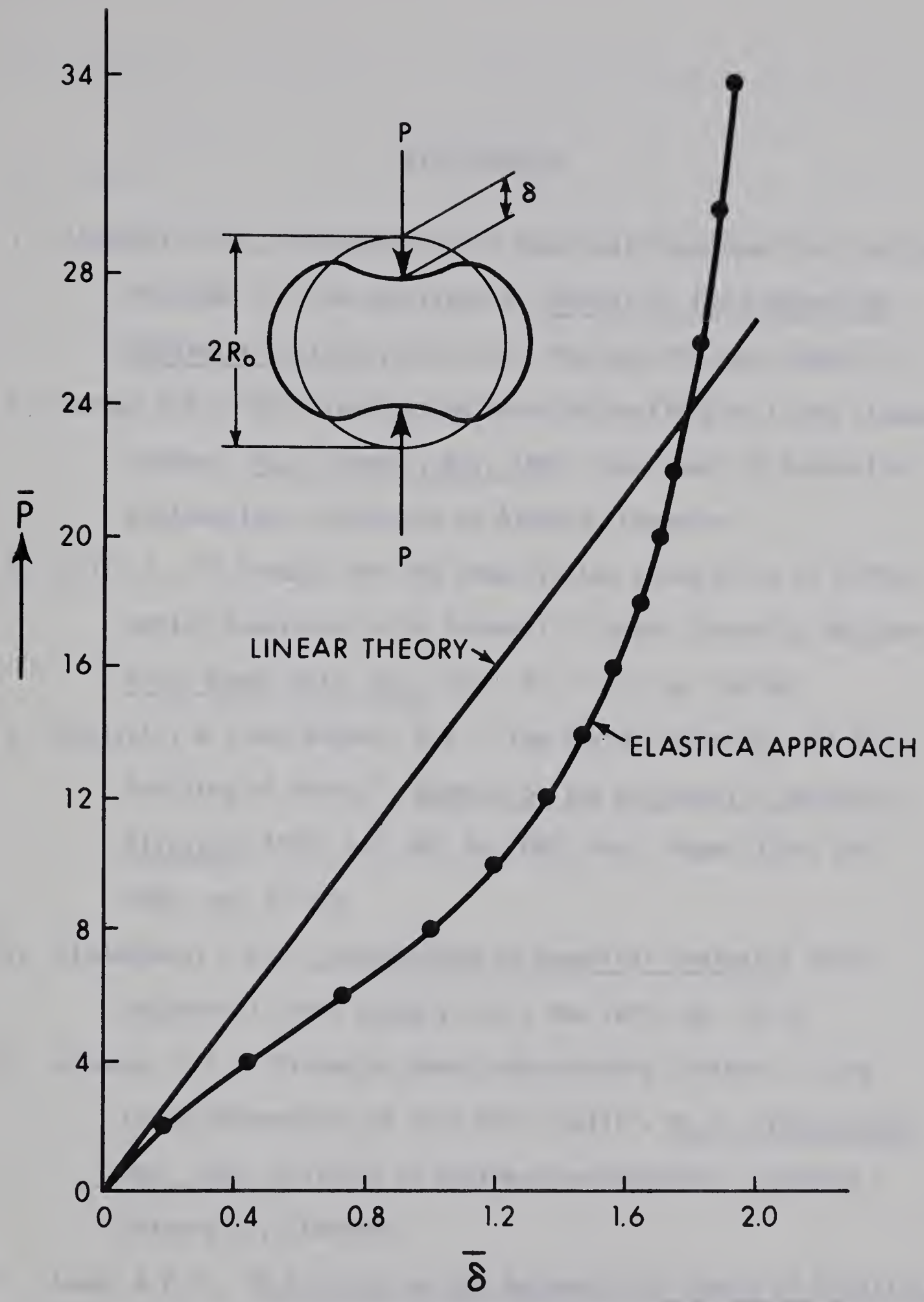

FIGURE 6.1 LOAD-DEFLECTION CURVES FOR A COMPLETE CIRCULAR RING LOADED BY TWO EQUAL DIAMETRICAL OPPOSED CONCENTRATED LOADS

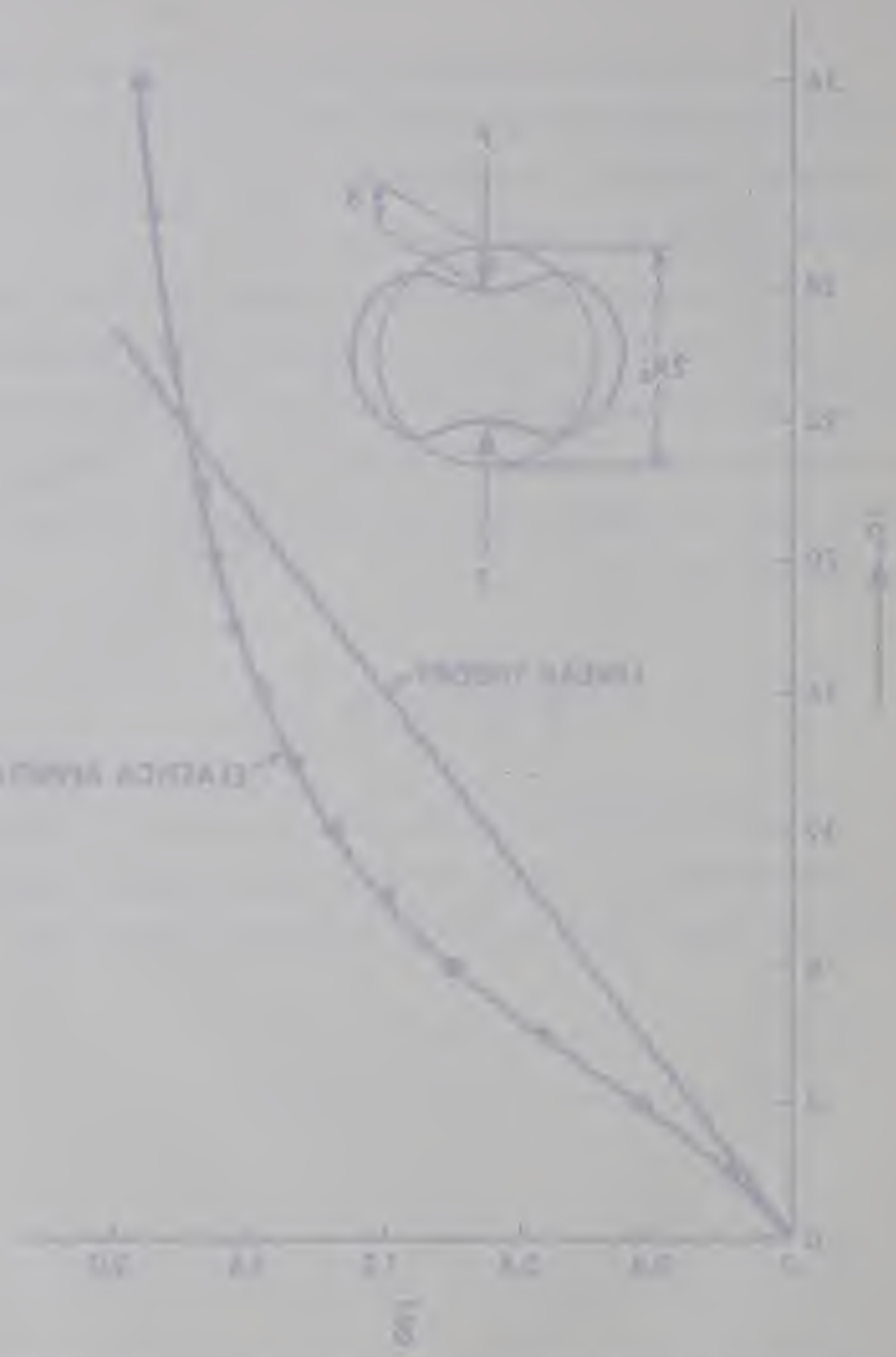

BIBLIOGRAPHY

1. Aggarwal, A.S., "Discussion on a Numerical Technique for Elastica Problems", To be published in Journal of the Engineering Mechanics Division, ASCE, Vol. 95, No. EM4, Aug. 1969.

2. Burns, D.A., "An Investigation into the Buckling of Light Clamped Arches", M.Sc. Thesis, Nov. 1963, Department of Mechanical Engineering, University of Alberta, Edmonton.

3. Gill, S., "A Process for the Step-By-Step Integration of Differential Equations in an Automatic Digital Computing Machine", Proc. Camb. Phil. Soc., Vol. 47, 1951, pp. 96-108.

4. Gjelsvik, A., and Bodner, S.R., "The Energy Criterion and Snap Buckling of Arches", Journal of the Engineering Mechanics Division, ASCE, Vol. 88, No. EM5, Proc. Paper 3304, Oct. 1962, pp. 87-134.

5. Hildebrand, F.B., "Introduction to Numerical Analysis", 1956, McGraw-Hill Book Company Inc., New York, pp. 72-76.

6. Kennedy, J.S., "Piecewise Nearly-Developable Surfaces in the Large Deformation of Very Thin Shells", Ph.D. Dissertation, Nov. 1959, Division of Engineering Mechanics, Stanford University, Stanford.

7. Love, A.E.H., "A Treatise on the Mathematical Theory of Elasticity", 1944, Dover Publications, New York, pp. 401-405.

8. Ralston, A., and Wilf, H.S., "Mathematical Methods for Digital Computers", 1960, John Wiley & Sons, Inc. New York.

9. Schreyer, H.L., and Masur, E.F., "Buckling of Shallow Arches", Journal of the Engineering Mechanics Division, ASCE, Vol. 92, No. EM4, Proc. Paper 4875, Aug. 1966, pp. 1-19.

10. Timoshenko, S.P., and Gere, J.M., "Theory of Elastic Stability", 1961, McGraw-Hill Book Company, Inc., New York.

APPENDIX A

NUMERICAL SOLUTION OF ORDINARY DIFFERENTIAL EQUATIONS

A.1 Introduction

The system of differential equations, 3.1, has been solved by Gill's variation of the Runge-Kutta Fourth Order method (8). This is a self starting integration procedure which is applicable to a system of n-first order ordinary differential equations and is highly suitable for use on a digital computer.

A.2 Runge-Kutta Methods

Given the system of first-order ordinary differential equations

$$\frac{dy_i}{dx} = y_i' = f_i(x, y_1(x), y_2(x), \ldots y_n(x))$$

with the initial conditions

$$y_i(x_o) = y_{io}$$

it is desired to obtain the values

$$y_i(x_o + h)$$

where h is an increment of the independent variable x.

The basis of all Runge-Kutta Methods is to express the difference between the values of y at x_{n+1} and x_n as

$$y_{n+1} - y_n = \sum_{i=1}^{m} c_i k_i$$

where c_i are constants and

$$k_i = h_n \, f(x_n + \alpha_i h_n, \, y_n + \sum_{j=1}^{i-1} \beta_{ij} k_j) \, .$$

c_i, α_i and β_{ij} are obtained to have desired properties by approximating the Taylor series solutions.

A.3 Gill's Modification

To apply, the method on high-speed digital computer, Gill (3) developed a calculation procedure in which the constants c_i, α_i, and β_{ij} are obtained to minimize the storage problem and to give the highest attainable accuracy. In addition, Gill's method requires comparatively few instructions and hence results in substantial savings in computer time. The calculation proceeds by sequentially calculating the j_n, k_n, and q_n values as given in Table A.1.

A.4 Accuracy of the Method

All the calculations are carried out in double-precision, that is carrying 16 significant figures. Therefore it is reasonable

Table A.1

Runge-Kutta Gill Scheme for First Order Differential Equation

$y' = f(x,y)$

x	j_n	q_n	$k_n = hf(x,j_n)$
x_o	$j_1 = y_o$		k_1
$x_o + \frac{h}{2}$	$j_2 = j_1 + \frac{1}{2} k_1$	$q_1 = k_1$	k_2
$x_o + \frac{h}{2}$	$j_3 = j_2 + (1 - \frac{1}{\sqrt{2}})(k_2 - q_1)$	$q_2 = (2 - \sqrt{2})\, k_2 + (-2 + \frac{3}{\sqrt{2}})q_1$	k_3
$x_o + h$	$j_4 = j_3 + (1 + \frac{1}{\sqrt{2}})(k_3 - q_2)$	$q_3 = (2 + \sqrt{2})\, k_3 + (-2 - \frac{3}{\sqrt{2}})q_2$	k_4

Then at $x_1 = x_o + h$

$$y_1 = j_4 + \frac{1}{6} k_4 - \frac{1}{3} q_3$$

to assume that round off errors are negligible.

The truncation errors in the process are caused because of neglecting terms $O(h^5)$ and higher in the Taylor Series expansion about the initial values. The evaluations of higher order terms is tedious. So it is not possible to estimate per step error. In order to overcome this disadvantage, control of accuracy is accomplished by adjusting the increment in x. A comparison is made between the function values obtained at $x = x_o + 2h$ by firstly using the increment h in two stages and secondly by using double the increment 2h in a single stage.

Let:

$c_1 h^5$ denote the truncation error using step h

$c_2(2h)^5$ denote the truncation error using step 2h

$y^{(1)}$ denote the value obtained at $x_o + 2h$ when using step h

$y^{(2)}$ denote the value obtained at $x_o + 2h$ when using step 2h

y denote the true value of y at $x_o + 2h$.

Then

$$y - y^{(1)} = 2 c_1 h^5$$

$$y - y^{(2)} = c_2(2h)^5$$

For small h, $c_1 \approx c_2$, therefore

$$y - y^{(1)} = \frac{1}{15}[y^{(2)} - y^{(1)}]$$

which gives a measure of the error introduced. To keep a check on the error, this procedure has been included in the integration procedure.

The introduced error $y - y^{(1)}$ is compared to the predefined accuracy (10^{-8} in the present problem) and if greater than desired, the step size h, is decreased. A Fortran IV subroutine DRKGS, based on the method described above is given in section A.5.

A.5 SUBROUTINE DRKGS

PURPOSE

TO SOLVE A SYSTEM OF FIRST ORDER ORDINARY DIFFERENTIAL EQUATIONS WITH GIVEN INITIAL VALUES.

USAGE

CALL DRKGS (PRMT,Y,DERY,NDIM,IHLF,FCT,OUTP,AUX)
PARAMETERS FCT AND OUTP REQUIRE AN EXTERNAL STATEMENT.

DESCRIPTION OF PARAMETERS

PRMT - DOUBLE PRECISION INPUT AND OUTPUT VECTOR WITH DIMENSION GREATER THAN OR EQUAL TO 5, WHICH SPECIFIES THE PARAMETERS OF THE INTERVAL AND OF ACCURACY AND WHICH SERVES FOR COMMUNICATION BETWEEN OUTPUT SUBROUTINE (FURNISHED BY THE USER) AND SUBROUTINE DRKGS. EXCEPT PRMT(5) THE COMPONENTS ARE NOT DESTROYED BY SUBROUTINE DRKGS AND THEY ARE

PRMT(1) - LOWER BOUND OF THE INTERVAL (INPUT),

PRMT(2) - UPPER BOUND OF THE INTERVAL (INPUT),

PRMT(3) - INITIAL INCREMENT OF THE INDEPENDENT VARIABLE (INPUT),

PRMT(4) - UPPER ERROR BOUND (INPUT). IF ABSOLUTE ERROR IS GREATER THAN PRMT(4), INCREMENT GETS HALVED. IF INCREMENT IS LESS THAN PRMT(3) AND ABSOLUTE ERROR LESS THAN PRMT(4)/50, INCREMENT GETS DOUBLED. THE USER MAY CHANGE PRMT(4) BY MEANS OF HIS OUTPUT SUBROUTINE.

PRMT(5) - NO INPUT PARAMETER. SUBROUTINE DRKGS INITIALIZES PRMT(5)=0. IF THE USER WANTS TO TERMINATE SUBROUTINE DRKGS AT ANY OUTPUT POINT, HE HAS TO CHANGE PRMT(5) TO NON-ZERO BY MEANS OF SUBROUTINE OUTP. FURTHER COMPONENTS OF VECTOR PRMT ARE FEASIBLE IF ITS DIMENSION IS DEFINED GREATER THAN 5. HOWEVER SUBROUTINE DRKGS DOES NOT REQUIRE AND CHANGE THEM. NEVERTHELESS THEY MAY BE USEFUL FOR HANDING RESULT VALUES TO THE MAIN PROGRAM (CALLING DRKGS) WHICH ARE OBTAINED BY SPECIAL MANIPULATIONS WITH OUTPUT DATA IN SUBROUTINE OUTP.

Y - DOUBLE PRECISION INPUT VECTOR OF INITIAL VALUES (DESTROYED). LATERON Y IS THE RESULTING VECTOR OF DEPENDENT VARIABLES COMPUTED AT INTERMEDIATE POINTS X.

DERY - DOUBLE PRECISION INPUT VECTOR OF ERROR WEIGHTS (DESTROYED). THE SUM OF ITS COMPONENTS MUST BE EQUAL TO 1. LATERON DERY IS THE VECTOR OF DERIVATIVES, WHICH BELONG TO FUNCTION VALUES Y AT INTERMEDIATE POINTS X.

NDIM - AN INPUT VALUE, WHICH SPECIFIES THE NUMBER OF EQUATIONS IN THE SYSTEM.

IHLF - AN OUTPUT VALUE, WHICH SPECIFIES THE NUMBER OF BISECTIONS OF THE INITIAL INCREMENT. IF IHLF GETS GREATER THAN 10, SUBROUTINE DRKGS RETURNS WITH ERROR MESSAGE IHLF=11 INTO MAIN PROGRAM. ERROR MESSAGE IHLF=12 OR IHLF=13 APPEARS IN CASE PRMT(3)=0 OR IN CASE SIGN(PRMT(3)).NE.SIGN(PRMT(2)-PRMT(1)) RESPECTIVELY.

FCT - THE NAME OF AN EXTERNAL SUBROUTINE USED. THIS SUBROUTINE COMPUTES THE RIGHT HAND SIDES DERY OF THE SYSTEM TO GIVEN VALUES X AND Y. ITS PARAMETER LIST MUST BE X,Y,DERY. SUBROUTINE FCT SHOULD NOT DESTROY X AND Y.

OUTP - THE NAME OF AN EXTERNAL OUTPUT SUBROUTINE USED. ITS PARAMETER LIST MUST BE X,Y,DERY,IHLF,NDIM,PRMT. NONE OF THESE PARAMETERS (EXCEPT, IF NECESSARY, PRMT(4),PRMT(5),...) SHOULD BE CHANGED BY SUBROUTINE OUTP. IF PRMT(5) IS CHANGED TO NON-ZERO, SUBROUTINE DRKGS IS TERMINATED.

AUX - DOUBLE PRECISION AUXILIARY STORAGE ARRAY WITH 8 ROWS AND NDIM COLUMNS.

REMARKS

THE PROCEDURE TERMINATES AND RETURNS TO CALLING PROGRAM, IF

(1) MORE THAN 10 BISECTIONS OF THE INITIAL INCREMENT ARE NECESSARY TO GET SATISFACTORY ACCURACY (ERROR MESSAGE IHLF=11),

(2) INITIAL INCREMENT IS EQUAL TO 0 OR HAS WRONG SIGN (ERROR MESSAGES IHLF=12 OR IHLF=13),

(3) THE WHOLE INTEGRATION INTERVAL IS WORKED THROUGH,

(4) SUBROUTINE OUTP HAS CHANGED PRMT(5) TO NON-ZERO.

SUBROUTINES AND FUNCTION SUBPROGRAMS REQUIRED

THE EXTERNAL SUBROUTINES FCT(X,Y,DERY) AND OUTP(X,Y,DERY,IHLF,NDIM,PRMT) MUST BE FURNISHED BY THE USER.

METHOD

EVALUATION IS DONE BY MEANS OF FOURTH ORDER RUNGE-KUTTA FORMULAE IN THE MODIFICATION DUE TO GILL. ACCURACY IS TESTED COMPARING THE RESULTS OF THE PROCEDURE WITH SINGLE AND DOUBLE INCREMENT.

SUBROUTINE DRKGS AUTOMATICALLY ADJUSTS THE INCREMENT DURING THE WHOLE COMPUTATION BY HALVING OR DOUBLING. IF MORE THAN 10 BISECTIONS OF THE INCREMENT ARE NECESSARY TO GET SATISFACTORY ACCURACY, THE SUBROUTINE RETURNS WITH ERROR MESSAGE IHLF=11 INTO MAIN PROGRAM.

TO GET FULL FLEXIBILITY IN OUTPUT, AN OUTPUT SUBROUTINE MUST BE FURNISHED BY THE USER.

```
      SUBROUTINE DRKGS(PRMT,Y,DERY,NDIM,IHLF,FCT,OUTP,AUX)

      DIMENSION Y(1),DERY(1),AUX(8,1),A(4),B(4),C(4),PRMT(1)
      DOUBLE PRECISION PRMT,Y,DERY,AUX,A,B,C,X,XEND,H,AJ,BJ,CJ,R1,R2,
     1DELT
      DO 1 I=1,NDIM
    1 AUX(8,I)=.06666666666666667D0*DERY(I)
      X=PRMT(1)
      XEND=PRMT(2)
      H=PRMT(3)
      PRMT(5)=0.D0
      CALL FCT(X,Y,DERY)
      ERROR TEST
      IF(H*(XEND-X))38,37,2

      PREPARATIONS FOR RUNGE-KUTTA METHOD
    2 A(1)=.5D0
      A(2)=.29289321881345248D0
      A(3)=1.7071067811865475D0
      A(4)=.16666666666666667D0
      B(1)=2.D0
      B(2)=1.D0
      B(3)=1.D0
      B(4)=2.D0
      C(1)=.5D0
      C(2)=.29289321881345248D0
      C(3)=1.7071067811865475D0
      C(4)=.5D0

      PREPARATIONS OF FIRST RUNGE-KUTTA STEP
      DO 3 I=1, NDIM
      AUX(1,I)=Y(I)
      AUX(2,I)=DERY(I)
      AUX(3,I)=0.D0
    3 AUX(6,I)=0.D0
      IREC=0
      H=H+H
      IHLF=-1
      ISTEP=0
      IEND=0

      START OF A RUNGE-KUTTA STEP
    4 IF((X+H-XEND)*H)7,6,5
    5 H=XEND-X
    6 IEND=1
```

```
    RECORDING OF INITIAL VALUES OF THIS STEP
 7  CALL OUTP(X,Y,DERY,IREC,NDIM,PRMT)
    IF(PRMT(5))40,8,40
 8  ITEST=0
 9  ISTEP=ISTEP+1


    START OF INNERMOST RUNGE-KUTTA LOOP
    J=1
10  AJ=A(J)
    BJ=B(J)
    CJ=C(J)
    DO 11 I=1,NDIM
    R1=H*DERY(I)
    R2=AJ*(R1-BJ*AUX(6,I))
    Y(I)=Y(I)+R2
    R2=R2+R2+R2
11  AUX(6,I)=AUX(6,I)+R2-CJ*R1
    IF(J-4)12,15,15
12  J=J+1
    IF(J-3)13,14,13
13  X=X+.5D0*H
14  CALL FCT(X,Y,DERY)
    GO TO 10
    END OF INNERMOST RUNGE-KUTTA LOOP


    TEST OF ACCURACY
15  IF(ITEST)16,16,20

    IN CASE ITEST=0 THERE IS NO POSSIBILITY FOR TESTING OF ACCURACY
16  DO 17 I=1, NDIM
17  AUX(4,I)=Y(I)
    ITEST=1
    ISTEP=ISTEP+ISTEP-2
18  IHLF=IHLF+1
    X=X-H
    H=.5D0*H
    DO 19 I=1, NDIM
    Y(I)=AUX(1,I)
    DERY(I)=AUX(2,I)
19  AUX(6,I)=AUX(3,I)
    GO TO 9

    IN CASE ITEST=1 TESTING OF ACCURACY IS POSSIBLE
20  IMOD=ISTEP/2
    IF(ISTEP-IMOD-IMOD)21,23,21
```

```
21  CALL FCT(X,Y,DERY)
    DO 22 I=1,NDIM
    AUX(5,I)=Y(I)
22  AUX(7,I)=DERY(I)
    GO TO 9

    COMPUTATION OF TEST VALUE DELT
23  DELT=0.D0
    DO 24 I=1,NDIM
24  DELT=DELT+AUX(8,I)*DABS(AUX(4,I)-Y(I))
    IF(DELT-PRMT(4))28,28,25

    ERROR IS TOO GREAT
25  IF(IHLF-10)26,36,36
26  DO 27 I=1,NDIM
27  AUX(4,I)=AUX(5,I)
    ISTEP=ISTEP+ISTEP-4
    X=X-H
    IEND=0
    GO TO 18

    RESULT VALUES ARE GOOD
28  CALL FCT(X,Y,DERY)
    DO 29 I=1,NDIM
    AUX(1,I)=Y(I)
    AUX(2,I)=DERY(I)
    AUX(3,I)=AUX(6,I)
    Y(I)=AUX(5,I)
29  DERY(I)=AUX(7,I)
    CALL OUTP(X-H,Y,DERY,IHLF,NDIM,PRMT)
    IF(PRMT(5))40,30,40
30  DO 31 I=1,NDIM
    Y(I)=AUX(1,I)
31  DERY(I)=AUX(2,I)
    IREC=IHLF
    IF(IEND)32,32,39

    INCREMENT GETS DOUBLED
32  IHLF=IHLF-1
    ISTEP=ISTEP/2
    H=H+H
    IF(IHLF)4,33,33
33  IMOD=ISTEP/2
    IF(ISTEP-IMOD-IMOD)4,34,4
34  IF(DELT-.02D0*PRMT(4))35,35,4
35  IHLF=IHLF-1
    ISTEP=ISTEP/2
    H=H+H
    GO TO 4
```

```
      RETURNS TO CALLING PROGRAM
   36 IHLF=11
      CALL FCT(X,Y,DERY)
      GO TO 39
   37 IHLF=12
      GO TO 39
   38 IHLF=13
   39 CALL OUTP(X,Y,DERY,IHLF,NDIM,PRMT)
   40 RETURN
      END
```

APPENDIX B

NUMERICAL INTEGRATION

B.1 Simpson's Rule

The solution of the system of differential equations, by the scheme described in Chapter III, gives the value of angle ϕ at equal intervals of $\bar{s}$. From this equal-interval data $\bar{x}$ and $\bar{y}$ given by the expressions

$$\bar{x} = \int_0^{\Omega} \cos\phi \, d\bar{s}$$

$$\bar{y} = \int_0^{\Omega} \sin\phi \, d\bar{s} \qquad \text{B.1}$$

are determined by the application of Simpson's Rule (5).

According to Simpson's Rule, the vector of integral values

$$z_i = z(x_i) = \int_a^{x_i} y(x) \, dx$$

$$(i = 1,2, \ldots, n)$$

with $x_i = a + (i - 1)h$

is given by

$$z_j = z_{j-2} + \frac{h}{3} (y_{j-2} + 4y_{j-1} + y_j) \qquad \text{B.2}$$

To use this formula, minimum three points are required.

B.2 Newton's Three-Eighth Rule

The major disadvantage of Simpson's Rule is that is requires the function values at odd number of points. This is overcome by employing it in combination with Newton's Three-Eighth Rule (5), which gives

$$z_j = z_{j-3} + \frac{3h}{8}(y_{j-3} + 3y_{j-2} + 3y_{j-1} + y_j) \qquad B.3$$

B.3 Accuracy of the Method

All the calculations are carried out in double-precision, that is carrying 16 significant figures. Therefore it is reasonable to assume that round off errors are negligible. Truncation error is of the order h^5 in both methods. The value of h used in the present problem is of the order 10^{-4}. Therefore truncation error too is negligible. A Fortran IV Subroutine DQSF, based on the method described above is given in section B.4.

B.4 SUBROUTINE DQSF

PURPOSE

TO COMPUTE THE VECTOR OF INTEGRAL VALUES FOR A GIVEN EQUIDISTANT TABLE OF FUNCTION VALUES.

USAGE

```
CALL DQSF (H,Y,Z,NDIM)
```

DESCRIPTION OF PARAMETERS

```
H     - DOUBLE PRECISION INCREMENT OF ARGUMENT VALUES.
Y     - DOUBLE PRECISION INPUT VECTOR OF FUNCTION VALUES.
Z     - RESULTING DOUBLE PRECISION VECTOR OF INTEGRAL
        VALUES.  Z MAY BE IDENTICAL WITH Y.
NDIM  - THE DIMENSION OF VECTORS Y AND Z.
```

REMARKS

NO ACTION IN CASE NDIM LESS THAN 3.

SUBROUTINES AND FUNCTION SUBPROGRAMS REQUIRED

NONE

METHOD

BEGINNING WITH Z(1)=0, EVALUATION OF VECTOR Z IS DONE BY MEANS OF SIMPSONS RULE TOGETHER WITH NEWTONS 3/8 RULE OR A COMBINATION OF THESE TWO RULES. TRUNCATION ERROR IS OF ORDER H**5 (I.E. FOURTH ORDER METHOD).

```
      SUBROUTINE DQSF(H,Y,Z,NDIM)


      DIMENSION Y(1), Z(1)
      DOUBLE PRECISION Y,Z,H,HT, SUM1, SUM2, AUX, AUX1, AUX2

      HT=.33333333333333333DO*H
      IF(NDIM-5)7,8,1

      NDIM IS GREATER THAN 5.  PREPARATIONS OF INTEGRATION LOOP
1     SUM1=Y(2)+Y(2)
      SUM1=SUM1+SUM1
      SUM1=HT*(Y(1)+SUM1+Y(3))
      AUX1=Y(4)+Y(4)
      AUX1=AUX1+AUX1
      AUX1=SUM1+HT*(Y(3)+AUX1+Y(5))
      AUX2=HT*(Y(1)+3.875DO*(Y(2)+Y(5))+2.625DO*(Y(3)+Y(4))+Y(6))
      SUM2=Y(5)+Y(5)
      SUM2=SUM2+SUM2
      SUM2=AUX2-HT*(Y(4)+SUM2+Y(6))
```

```
      Z(1)=0.D0
      AUX=Y(3)+Y(3)
      AUX=AUX+AUX
      Z(2)=SUM2-HT*(Y(2)+AUX+Y(4))
      Z(3)=SUM1
      Z(4)=SUM2
      IF(NDIM-6)5,5,2
      INTEGRATION LOOP
2     DO 4 I=7,NDIM,2
      SUM1=AUX1
      SUM2=AUX2
      AUX1=Y(I-1)+Y(I-1)
      AUX1=AUX1+AUX1
      AUX1=SUM1+HT*(Y(I-2)+AUX1+Y(I))
      Z(I-2)=SUM1
      IF(I-NDIM)3,6,6
3     AUX2=Y(I)+Y(I)
      AUX2=AUX2+AUX2
      AUX2=SUM2+HT*(Y(I-1)+AUX2+Y(I+1))
4     Z(I-1)=SUM2
5     Z(NDIM-1)=AUX1
      Z(NDIM)=AUX2
      RETURN
6     Z(NDIM-1)=SUM2
      Z(NDIM)=AUX1
      RETURN
      END OF INTEGRATION LOOP

 7    IF(NDIM-3)12,11,8

      NDIM IS EQUAL TO 4 OR 5
 8    SUM2=1.125D0*HT*(Y(1)+Y(2)+Y(2)+Y(2)+Y(3)+Y(3)+Y(3)+Y(4))
      SUM1=Y(2)+Y(2)
      SUM1=SUM1+SUM1
      SUM1=HT*(Y(1)+SUM1+Y(3))
      Z(1)=0.D0
      AUX1=Y(3)+Y(3)
      AUX1=AUX1+AUX1
      Z(2)=SUM2-HT*(Y(2)+AUX1+Y(4))
      IF(NDIM-5)10,9,9
 9    AUX1=Y(4)+Y(4)
      AUX1=AUX1+AUX1
      Z(5)=SUM1+HT*(Y(3)+AUX1+Y(5))
10    Z(3)=SUM1
      Z(4)=SUM2
      RETURN
```

```
      NDIM IS EQUAL TO 3
11    SUM1=HT*(1.25D0*Y(1)+Y(2)+Y(2)-.25D0*Y(3))
      SUM2=Y(2)+Y(2)
      SUM2=SUM2+SUM2
      Z(3)=HT*(Y(1)+SUM2+Y(3))
      Z(1)=0.D0
      Z(2)=SUM1
12    RETURN
      END
```